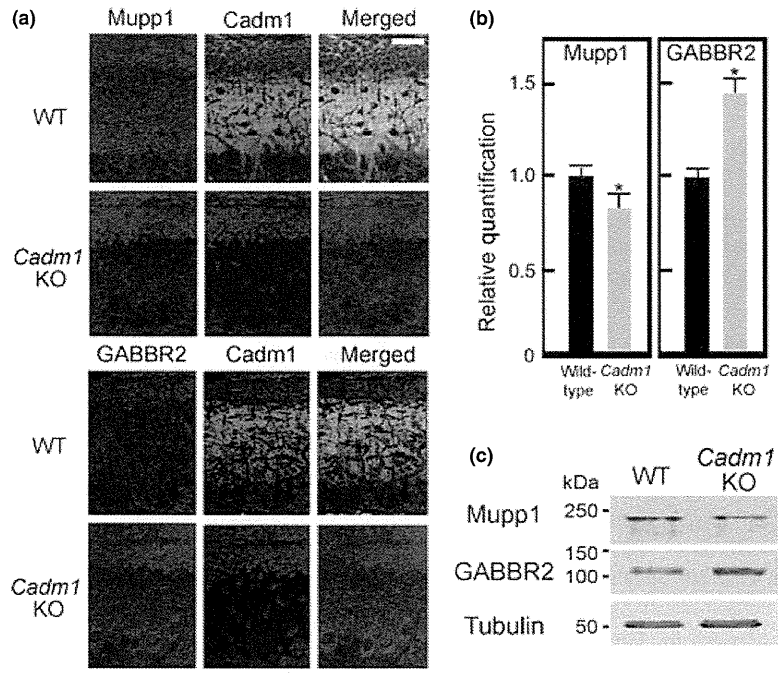

Fig. 5 Alteration of gamma-aminobutyric acid type B receptor (GABBR)2 immunoreactivity in the cerebellum of *Cadm1*-KO mice (P 11). (a) Anti-Cadm1 (green) and anti-Mupp1 or anti-GABBR2 (red) visualized in the cerebellum of wild-type (WT) mice. Cell adhesion molecule 1 (Cadm1) and multiple PDZ domain protein 1 (Mupp1) were preferentially distributed in the distal-apical dendritic portion and the proximal dendritic region of the WT mice, respectively, but the Mupp1 intensity gradient was lost in the *Cadm1*-KO mice. Compared with WT, GABBR2 intensity increased in the molecular layer of the *Cadm1*-KO mice. Nuclei were stained with Hoechst (blue). Bar, 30 μm. To eliminate variations because of regional differences, sections were taken from the same region in the central part of the cerebella of the WT and homozygous *Cadm1*-KO mice. (b) The intensities of Mupp1 and/or GABBR2 in the WT and *Cadm1*-KO mice. Values are mean ± standard error (SEM). Student's *t*-test (*$p < 0.05$). Pups: $n = 3$. Images: $n = 8$. (c) Immunoblot analysis of the alteration of the GABBR2 level in the cerebella of WT and *Cadm1*-KO mice with anti-Mupp1, anti-GABBR2, and anti-Tubulin.

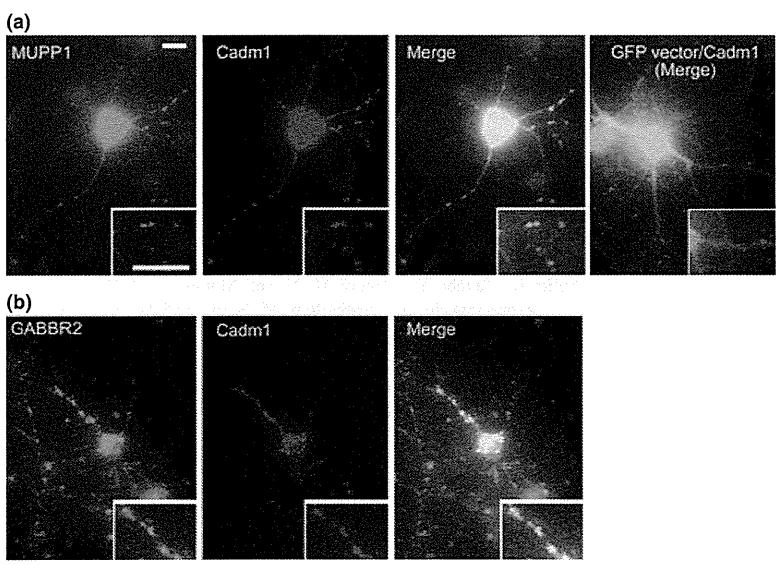

Fig. 6 Localization of cell adhesion molecule 1 (Cadm1)-C, multiple PDZ domain protein 1 (Mupp1), and gamma-aminobutyric acid type B receptor (GABBR) 2 in hippocampal neurons. Cadm1–myc and GFP–Mupp1 or GFP alone (a), or Cadm1–myc and GABBR2 (b) were cotransfected into hippocampal neurons and their intracellular colocalization was visualized with anti-GFP or anti-GABBR2 and anti-myc. Bar indicates 20 μm.

© 2012 The Authors

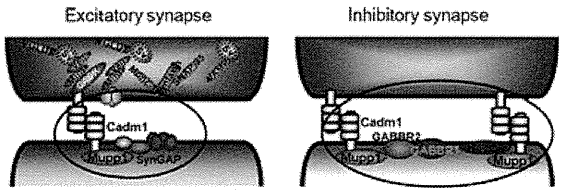

Fig. 7 Possible model for cell adhesion molecule 1 (Cadm1)–multiple PDZ domain protein 1 (Mupp1)–gamma-aminobutyric acid type B receptor (GABBR)2 complex at the post-synaptic membrane.

to speech–language disorder (Fujita *et al.* 2008, 2012a). In contrast with *Cadm1*-KO pups, *Foxp2*(R552H)-KI pups carry a reduced number of synapses expressing Cadm1 and GABBR2 on the dendrites of Purkinje cells, whereas more GABBR2 occurs in the cerebella of *Cadm1*-KO mice. Furthermore, the NLGN3(R451C) mutation is found in ASD patients, and GABAergic transmission is increased in *Nlgn3 (R451C)*-KI mice (Tabuchi *et al.* 2007), suggesting that GABBR2 up-regulation may not be related to the impaired USVs, but rather to other ASD-like symptoms of *Cadm1*-KO mice. The relationship between the physiological alteration of the Cadm–Mupp1-receptor complex and the impaired social interactions of *Cadm1*-KO mice, a symptom of ASD, will be a major focus of future study.

In conclusion, Cadm1 associated with Mupp1 at PDZ(1-5) and colocalized with Mupp1 and GABBR2 in the molecular layer of the cerebellum. Lack of Cadm1 increased the up-regulation of GABBR2 in the cerebellum. Cadm1 may therefore form a ternary complex with Mupp1–GABBR2 in the cerebellum.

Acknowledgements

This work was supported by Grants-in-Aid for Scientific Research (KAKENHI) of the Ministry of Education, Culture, Sports, Science and Technology, Japan (21200011, 21700377); Grants-in-Aid for Health Labour Scientific Research of the Ministry of the Health, Labour and Welfare, Japan (10103243). We are extremely grateful to all the families. We thank Dr. S. Tsukita, Dr. C. Ullmer, and Dr. A.E. El-Hussini for providing cDNA. The authors declare no conflict of interest.

Supporting information

Additional supporting information may be found in the online version of this article:

Figure S1. The expression of Mupp1 and GABBR2 in the cerebellum of wild-type and *Cadm1*KO mice (P10).

As a service to our authors and readers, this journal provides supporting information supplied by the authors. Such materials are peer-reviewed and may be re-organized for online delivery, but are not copy-edited or typeset. Technical support issues arising from supporting information (other than missing files) should be addressed to the authors.

References

Balasubramanian S., Fam S. R. and Hall R. A. (2007) GABBReceptor association with the PDZ scaffold Mupp 1 alters receptor stability and function. *J. Biol. Chem.* **282**, 4162–4171.

Bauman M. L. and Kemper T. L. (1994) Neuroanatomic observations of the brain in autism, in *The Neurobiology of Autism*, (Bauman M. L. and Kemper T. L., eds), pp. 19–145. Johns Hopkins University Press, Baltimore.

Becamel C., Figge A., Poliak S., Dumuis A., Peles E., Bockaert J., Lubbert H. and Ullmer C. (2001) Interaction of serotonin 5-hydroxytryptamine type 2C receptors with PDZ10 of the multi-PDZ domain protein MUPP1. *J. Biol. Chem.* **276**, 12974–12982.

Biederer T., Sara Y., Mozhayeva M., Atasoy D., Liu X., Kavalali E. T. and Südhof T. C. (2002) SynCAM, a synaptic adhesion molecule that drives synapse assembly. *Science* **297**, 1525–1531.

Branchi I., Santucci D. and Alleva E. (2001) Ultrasonic vocalisation emitted by infant rodents: a tool for assessment of neurobehavioural development. *Behav. Brain Res.* **125**, 49–56.

Fatemi S. H., Halt A. R., Realmuto G., Earle J., Kist D. A., Thuras P. and Merz A. (2000) Purkinje cell size is reduced in cerebellum of patients with autism. *Cell. Mol. Neurobiol.* **22**, 171–175.

Fujita E., Soyama A. and Momoi T. (2003) RA175, which is the mouse ortholog of TSLC1, a tumor suppressor gene in human lung cancer, is a cell adhesion molecule. *Exp. Cell Res.* **287**, 57–66.

Fujita E., Urase K., Soyama A., Kouroku Y. and Momoi T. (2005) Distribution of RA175/TSLC1/SynCAM, a member of the immunoglobulin superfamily, in the developing nervous system. *Brain Res. Dev. Brain Res.* **154**, 199–209.

Fujita E., Kouroku Y., Ozeki S., Tanabe Y., Toyama Y., Maekawa M., Kojima N., Senoo H., Toshimori K. and Momoi T. (2006) Oligo-astheno-teratozoospermia in mice lacking RA175/TSLC1/SynCAM/IGSF4A, a cell adhesion molecule in the immunoglobulin superfamily. *Mol. Cell. Biol.* **26**, 718–726.

Fujita E., Tanabe Y., Hirose T., Aurrand-Lions M., Kasahara T., Imhof B. A., Ohno S. and Momoi T. (2007) Loss of partitioning-defective-3/isotype-specific interacting protein (par-3/ASIP) in the elongating spermatid of RA175 (IGSF4A/SynCAM)-deficient mice. *Am. J. Pathol.* **171**, 1800–1810.

Fujita E., Tanabe Y., Shiota A., Ueda M., Suwa K., Momoi M. Y. and Momoi T. (2008) Ultrasonic vocalization impairment of Foxp2 (R552H) knockin mice related to speech-language disorder and abnormality of Purkinje cells. *Proc. Natl Acad. Sci. USA* **105**, 3117–3122.

Fujita E., Dai H., Tanabe Y., Zhiling Y., Yamagata T., Miyakawa T., Tanokura M., Momoi M. Y. and Momoi T. (2010) Autism spectrum disorder is related to endoplasmic reticulum stress induced by mutations in the synaptic cell adhesion molecule, CADM1. *Cell Death Dis.* **1**, e47.

Fujita E., Tanabe Y., Imhof B. A., Momoi M. Y. and Momoi T. (2012a) Cadm1 at synapses on the dendrites of Purkinje cells is involved in mouse ultrasonic vocalization activity. *PLoS ONE* **7**, e30151.

Fujita E., Tanabe Y., Momoi M. Y. and Momoi T. (2012b) Cntnap2 expression in the cerebellum of Foxp2(R552H) mice, with a mutation related to speech-language disorder. *Neurosci. Lett.* **506**, 277–280.

Gerrow K. and El-Husseini A. (2007) Receptors look outward: revealing signals that bring excitation to synapses. *Sci. STKE* **408**, e56.

Goslin K. and Banker G.. (1998) Rat hippocampal neurons in low density culture, in *Culturing Nerve Cells* (Banker G. and Goslin K., eds), pp. 251–282. MIT, Cambridge.

Hamazaki Y., Itoh M., Sasaki H., Furuse M. and Tsukita S. (2002) Multi-PDZ domain protein 1 (MUPP1) is concentrated at tight

© 2012 The Authors

junctions through its possible interaction with claudin-1 and junctional adhesion molecule. *J. Biol. Chem.* **277**, 455–461.

Horresh I., Poliak S., Grant S., Bredt D., Rasband M. N. and Peles E. (2008) Multiple molecular interactions determine the clustering of Caspr2 and Kv1 channels in myelinated axons. *J. Neurosci.* **28**, 14213–14222.

Kraplvinsky G., Medina I., Kraplvinsky L., Gapon S. and Clapham D. E. (2004) SynGAP-Mupp 1-CaMKII synaptic complexes regulate p38 MAP kinase activity and NMDA receptor dependent synaptic AMPA receptor potentiation. *Neuron* **43**, 563–574.

Luján R. and Shigemoto R. (2006) Localization of metabotropic GABA receptor subunits GABAB1 and GABAB2 relative to synaptic sites in the rat developing cerebellum. *Eur. J. Neurosci.* **23**, 1479–1490.

Miyazaki T., Fukaya M., Shimizu H. and Watanabe M. (2003) Subtype switching of vesicular glutamate transporters at parallel fibre-Purkinje cell synapses in developing mouse cerebellum. *Eur. J. Neurosci.* **17**, 2563–2572.

Pickett J. and London E. (2005) The neuropathology of autism. *J. Neuropathol. Exp. Neurol.* **64**, 925–935.

Ritvo E. R., Freeman B. J., Scheibel A. B., Duong T., Robinson H., Guthrie D. and Ritvo A. (1986) Lower Purkinje cell counts in the cerebella of four autistic subjects: initial findings of the UCLA-NSAC autopsy research report. *Am. J. Psychiatry* **143**, 862–866.

Sala C., Piëch V., Wilson N. R., Passafaro M., Liu G. and Sheng M. (2001) Regulation of dendritic spine morphology and synaptic function by Shank and Homer. *Neuron* **31**, 115–130.

Sitek B., Poschmann G., Schmidtke K., Ullmer C., Maskri L., Andriske M., Stichel C. C., Zhu X. R. and Luebbert H. (2003) Expression of MUPP1 protein in mouse brain. *Brain Res.* **970**, 178–187.

Tabuchi K., Blundell J., Etherton M. R., Hammer R. E., Liu X., Powell C. M. and Südhof T. C. (2007) A neuroligin-3 mutation implicated in autism increases inhibitory synaptic transmission in mice. *Science* **318**, 71–76.

Takayanagi Y., Fujita E., Yu Z., Yamagata T., Momoi M. Y., Momoi T. and Onaka T. (2010) Impairment of social and emotional behaviors in Cadm1-knockout mice. *Biochem. Biophys. Res. Commun.* **396**, 703–708.

Urase K., Soyama A., Fujita E. and Momoi T. (2001) Expression of RA175 mRNA, a new member of the immunoglobulin superfamily, in developing mouse brain. *NeuroReport* **12**, 3217–3221.

Zhiling Y., Fujita E., Tanabe Y., Yamagata T., Momoi T. and Momoi M. Y. (2008) Mutations in the gene encoding CADM1 are associated with autism spectrum disorder. *Biochem. Biophys. Res. Commun.* **377**, 926–929.

© 2012 The Authors

OPEN ACCESS Freely available online

PLoS one

Cadm1-Expressing Synapses on Purkinje Cell Dendrites Are Involved in Mouse Ultrasonic Vocalization Activity

Eriko Fujita[1,2], Yuko Tanabe[1], Beat A. Imhof[3], Mariko Y. Momoi[2]*, Takashi Momoi[1]*

1 Center for Medical Science, International University of Health and Welfare, Kitakanemaru, Ohtawara, Tochigi, Japan, **2** Department of Pediatrics, Jichi Medical University, Yakushiji, Shimotsukeshi, Tochigi, Japan, **3** Department of Pathology and Immunology, Centre Médical Universitaire, University of Geneva, Geneva, Switzerland

Abstract

Foxp2(R552H) knock-in (KI) mouse pups with a mutation related to human speech–language disorders exhibit poor development of cerebellar Purkinje cells and impaired ultrasonic vocalization (USV), a communication tool for mother-offspring interactions. Thus, human speech and mouse USV appear to have a Foxp2-mediated common molecular basis in the cerebellum. Mutations in the gene encoding the synaptic adhesion molecule CADM1 (RA175/Necl2/SynCAM1/Cadm1) have been identified in people with autism spectrum disorder (ASD) who have impaired speech and language. In the present study, we show that both *Cadm1*-deficient knockout (KO) pups and *Foxp2*(R552H) KI pups exhibit impaired USV and smaller cerebellums. Cadm1 was preferentially localized to the apical–distal portion of the dendritic arbor of Purkinje cells in the molecular layer of wild-type pups, and VGluT1 level decreased in the cerebellum of *Cadm1* KO mice. In addition, we detected reduced immunoreactivity of Cadm1 and VGluT1 on the poorly developed dendritic arbor of Purkinje cells in the *Foxp2*(R552H) KI pups. However, Cadm1 mRNA expression was not altered in the *Foxp2*(R552H) KI pups. These results suggest that although the Foxp2 transcription factor does not target Cadm1, Cadm1 at the synapses of Purkinje cells and parallel fibers is necessary for USV function. The loss of Cadm1-expressing synapses on the dendrites of Purkinje cells may be associated with the USV impairment that *Cadm1* KO and *Foxp2*(R552H) KI mice exhibit.

Citation: Fujita E, Tanabe Y, Imhof BA, Momoi MY, Momoi T (2012) Cadm1-Expressing Synapses on Purkinje Cell Dendrites Are Involved in Mouse Ultrasonic Vocalization Activity. PLoS ONE 7(1): e30151. doi:10.1371/journal.pone.0030151

Editor: Michael A. Fox, Virginia Commonwealth University Medical Center, United States of America

Received June 9, 2011; **Accepted** December 11, 2011; **Published** January 17, 2012

Copyright: © 2012 Fujita et al. This is an open-access article distributed under the terms of the Creative Commons Attribution License, which permits unrestricted use, distribution, and reproduction in any medium, provided the original author and source are credited.

Funding: This work was supported by Grants-in-Aid for Scientific Research (KAKENHI) of the Ministry of Education, Culture, Sports, Science and Technology, Japan (21200011, 21700377), Grants-in-Aid for Health Labour Scientific Research of the Ministry of the Health, Labour and Welfare, Japan (10103243). We are extremely grateful to all the families. The funders had no role in study design, data collection and analysis, decision to publish, or preparation of the manuscript.

Competing Interests: The authors have declared that no competing interests exist.

* E-mail: momoi@iuhw.ac.jp (TM); mymomoi@jichi.ac.jp (MM)

Introduction

Cadm1 (also known as RA175, Necl2, and SynCAM1), a member of the immunoglobulin superfamily (IgSF), localizes to both sides of the synaptic cleft and functions as a synaptic cell–cell adhesion molecule. Cadm1 induces functional synapses [1]. The extracellular domain of Cadm1 mediates calcium-independent, homophilic *trans* interactions [1,2], and its cytoplasmic tail has a band 4.1 region and a PSD95/Dlg/ZO-1 (PDZ)–binding motif [2]. At the pre-synapse, Cadm1 associates with calmodulin associated serine/threonine kinase (CASK) via a single PDZ domain [1].

Mutations in genes encoding synaptic adhesion proteins, including *neuroligin* (*NLGN*) 3 and 4, *contactin-associated protein-like 2* (*CNTNAP2*, *Caspr2*), and *CADM1*, are associated with autism spectrum disorder (ASD) [3–5]; the CADM1 mutations H246N and Y251S specifically have been found in people diagnosed with ASD who had impaired social interactions and communication, including speech and language impairments [5]. Mutations in CADM1 increase its susceptibility to processing errors and the accumulation of CADM1 peptide fragments in the endoplasmic reticulum [5,6]; they also reduce CADM1 affinity in cell adhesion and lead to synaptic defects in neuron cultures [6]. *Cadm1* knockout (KO) mice [7] exhibit abnormal social and emotional behaviors that share similarities with some behaviors associated with ASD [8]. These findings suggest that CADM1 loss of function may be linked to ASD.

Speech–language impairment is one of the most prominent symptoms in some types of ASD. Impaired speech–language communication frequently also occurs as a phenotype of people with mutations in the adhesion molecule gene *CNTNAP2* [4]. A previous study found an R553H mutation in human *FOXP2* in patients with speech–language disorders [9]. Normal FOXP2 associates with a corepressor and acts as a transcriptional repressor [10]; however, mutated FOXP2 (R553H) lacks DNA-binding activity [11]. Infant mice emit and use ultrasonic vocalizations (USVs) as an essential communication tool for mother–offspring interactions [12]. *Foxp2* KO mice and knock-in (KI) mice for *Foxp2* (R552H), which corresponds to the human *FOXP2* (R553H) mutation, exhibit severe USV impairments, suggesting human speech and mouse USVs may have a common molecular basis in the brain [13,14]. *Foxp2*(R552H) KI pups with USV impairment show poor development of Purkinje cells in the cerebellum [13], and the number of synapses on the dendrites of Purkinje cells is decreased in the these pups.

Of interest, cerebellar abnormalities, including Purkinje cell loss, have been found in autopsy samples from ASD patients [15]. We have observed that *Cadm1* KO mice have smaller cerebellums. Furthermore, Cadm1 mRNA is expressed not only in various regions of the cerebrum but also in the developing cerebellum [16]. Cadm1 is predominantly localized to the thalamus cortical afferent pathway in the cerebrum [17]; however, little is known about Cadm1 expression at synapses in the cerebellum.

In the present study, we examined USV of *Cadm1* KO mice, Cadm1 localization in the cerebellum, and the relationship between loss of Cadm1 at the synapses and impaired USV in *Cadm1* KO and *Foxp2*(R552H) KI pups.

Results

We established a strain of *Cadm1* KO (C57BL/6J) mice (*Cadm1* KO mice) by mating heterozygous *Cadm1* KO (129Sv) mice [7] with C57BL/6J for more than 10 generations. The homozygous *Cadm1* KO mice (postnatal day [P] 50) were smaller than their wild-type counterparts (Figure 1A). At P10, we detected a significant difference in mean body weight between homozygous *Cadm1* KO mice and their wild-type littermates, a difference that increased over the next 20 days. The mean body weight of the homozygous *Cadm1* KO mice was 20–25% less than that of the wild-type mice (Figure 1B). In addition, compared to the wild-type mice, the brains of homozygous *Cadm1* KO mice were smaller (Figure 1C). In particular, the cerebellum of homozygous *Cadm1* KO mice showed a reduction in size (Figure 1D, upper panel) and weight (Figure 1D, lower panel) of approximately 20%.

We next investigated the pups' USV because we previously found poor development of Purkinje cells in *Foxp2*(R552H) KI mice with impaired USV [13]. The *Cadm1* KO pups exhibited impaired USV upon separation from their mothers and litters, an effect similar to that which we recently observed in *Foxp2*(R552H) KI pups (Figure 2A) [13]. The *Cadm1* KO pups produced some click-type USVs but only low levels of whistle-type USVs, compared to the predominant whistle-type USVs among wild-type pups (Figure 2B, C).

The detection of these functional effects associated with Cadm1 deficiency led us to investigate more thoroughly the distribution pattern of Cadm1 in the cerebellum. In P11 wild-type pups, but not *Cadm1* KO pups, Cadm1 was detected in the dendritic arbor of Purkinje cells and some of the granular cells in the cerebellum (Figure 3A). Cadm1 preferentially localized to the apical–distal portion of the dendritic arbor (Figure 3B). The dendrite development of Purkinje cells in *Cadm1* KO mice appeared poor compared to that of wild-type mice (Figure 3B and Figure S1).

Purkinje cells receive two excitatory afferents, parallel fibers and climbing fibers, which can be distinguished based on the expression of VGluT1 and VGluT2 [18,19]; climbing fibers express VGluT2 throughout development while parallel fibers shift from VGluT2 expression to VGluT1. The onset of VGluT2 expression in the individual parallel fiber terminals was clearly earlier than that of VGluT1 in the samples; in the early postnatal stages (P6–8), Cadm1 was mainly expressed in the molecular layer with the expression of VGluT2 (Figure 4A). During P6–11, Cadm1 expression intensity increased. At P11, VGluT2 intensity decreased, while VGluT1 intensity increased (Figure 4B). Thus, VGluT2 in parallel fibers expressing Cadm1 was replaced with VGluT1, which extended its expression from proximal regions to apical–distal regions in the molecular layer (Figure 4A). After this deep-to-superficial replacement, Cadm1 and VGluT1 immunoreactivity was detected throughout the molecular layer and appeared to co-localize at P14 (Figure 4A).

We next examined the levels of Foxp2, Synaptophysin, and VGluT1 in the cerebellum of *Cadm1* KO mice (Figure 5A). VGluT1 levels were markedly decreased in the cerebellum of *Cadm1* KO compared to wild-type mice. Compared to VGluT1, the decrease in

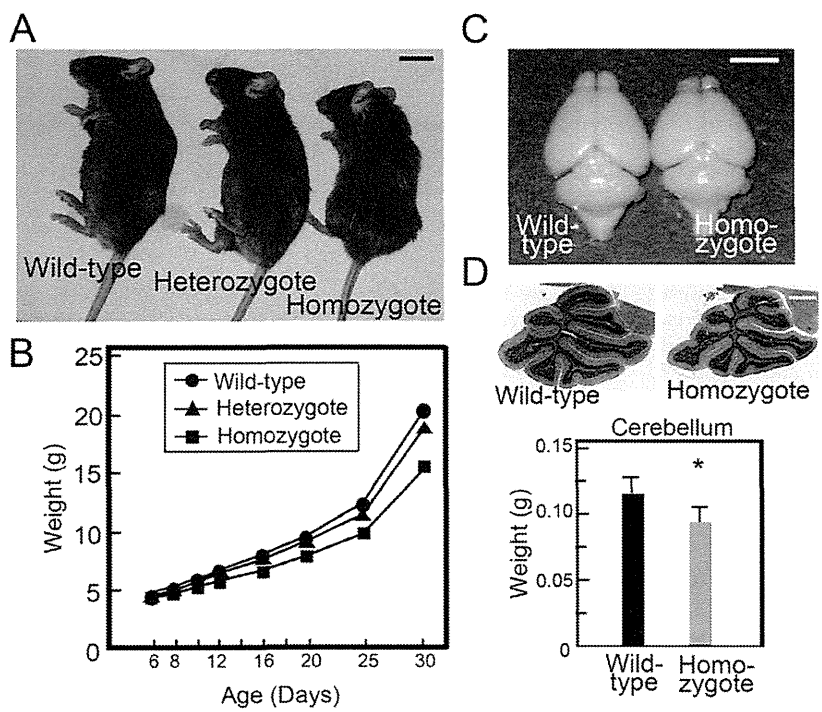

Figure 1. Abnormal cerebellum development of *Cadm1* KO. (A) Wild-type, heterozygote, and homozygous *Cadm1* KO mice. (P50) (B) The difference in mean weight between homozygous *Cadm1* KO mice and their wild-type littermates (five each) was significant at P10 and increased over the next 20 days (A, B); at P30, the mean weight of the homozygous *Cadm1* KO mice was 20–25% less than that of the wild-type mice. In addition, the brains of homozygous *Cadm1* KO mice were smaller (C, n = 22), and the cerebellums of homozygous *Cadm1* KO mice had an approximately 20% reduction in size and weight (D, n = 10). Bars in the graph indicate mean ± standard error (SEM). Student's *t*-test (*$p<0.05$). Bars in the pictures indicate 1 cm (A), 5 mm (C), and 0.75 mm (D), respectively.
doi:10.1371/journal.pone.0030151.g001

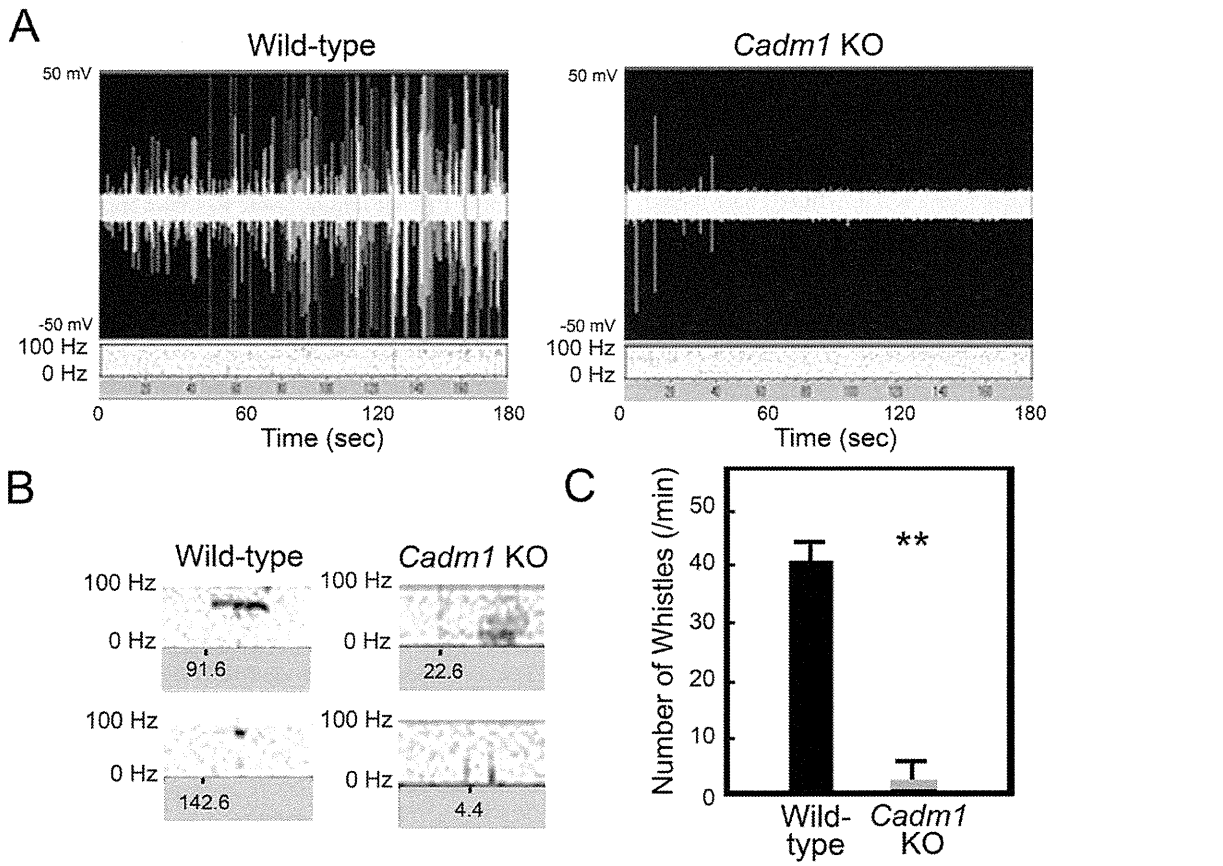

Figure 2. Analysis of ultrasonic vocalizations (USVs) of *Cadm1* KO mice (P8). (A) Real-time spectrography of the USVs by pups after separation from the dam. (B) Major vocalization patterns of *Cadm1* KO and wild-type pups. Wild-type vocalization was mainly whistle-type USVs, but *Cadm1* KO mice exhibited only a small number of click-type vocalizations. (C) The number of whistle-type USVs per min by pups. Vocalizations were recorded for 3 min. Experiments were done three times for 5 pups in each group, and an example of typical results is shown. Values are mean±standard error (SEM). Student's *t*-test (**$p<0.01$).
doi:10.1371/journal.pone.0030151.g002

Synaptophysin was not marked, but it was significant; however, Foxp2 levels were unchanged. Real-time PCR analysis confirmed that there was no alteration in Foxp2 mRNA levels in the cerebellum of *Cadm1* KO compared to wild-type mice (Figure 5B).

Thus, Cadm1 deficiency did not appear to affect *Foxp2* expression and Foxp2-mediated development of Purkinje cell dendrites; however, it may have influenced synapse formation.

We also examined the localization of Cadm1 in the cerebellum of *Foxp2*(R552H) KI mice and found that *Foxp2*(R552H) KI pups (P11) had poorly developed Purkinje cell dendrites with reduced immunoreactivity for Synaptophysin [13] (Figure 6). Overall, the immunoreactivity of Cadm1, as well as of VGluT1, was reduced on dendritic arbors in *Foxp2*(R552H) KI mice (Figure 6 and Figure S2), although Cadm1 mRNA levels were unchanged (Figure S3).

Discussion

Foxp2-mediated USV and Cadm1 activity in synapses in the cerebellum

Human speech and mouse USV have a common molecular basis in the brain, and *Foxp2*(R552H) KI mice exhibit abnormal cerebellar development and poor dendrite development [13]. In humans, some of the areas associated with speech and language skills are located in the frontal/superior cerebellar articulation control system and the parietal/inferior cerebellar phonological storage system [20,21]. The cerebellar molecular systems control both human spoken language and mouse USVs and therefore share function in the two species.

In the present study, we found that *Cadm1* KO mice had smaller cerebellums, poor development of dendrites of Purkinje cells, and impaired USV (Figures 1, 2, 3 and S1), as observed in *Foxp2*(R552H) KI mouse pups. Cadm1 was preferentially localized to the apical–distal portion of the dendritic arbor of Purkinje cells in the molecular layer of wild-type pups (Figure 3), and the level of VGluT1 decreased in the cerebellum of *Cadm1* KO mice (Figure 5).

VGluT1/2-positive synapses have been detected in the brains of transgenic mice overexpressing *Cadm1* [22]. In the cerebellum, the two excitatory afferents of Purkinje cells are the parallel fibers and climbing fibers; climbing fiber terminals selectively express VGluT2 throughout the postnatal period, but parallel fiber terminals first express VGluT2 and then switch to VGluT1 [18,19]. In the current work, Cadm1 was expressed in the granular cells and appeared to co-localize with VGluT1 at the presynapse (Figure 4). Both Cadm1 and VGluT1 immunoreactivity decreased in the Purkinje cells of *Foxp2*(R552H) KI pups (P11) with impaired USV (Figure 6), however. Of note, Cadm1

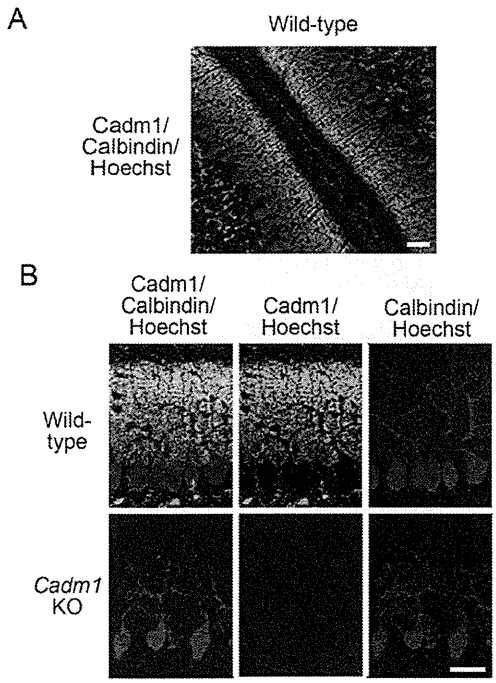

Figure 3. Distribution of Cadm1 in the cerebellum (P11). The Cadm1 intensity preferentially distributed in an apical–distal dendritic portion. Wild-type (A, B, upper panel) and *Cadm1* KO mice (B, lower panel). Green, Cadm1. Red, Calbindin. Blue, Hoechst. Bars, 30 μm.
doi:10.1371/journal.pone.0030151.g003

homophilically *trans* interacts at the synapse [1,2]. In this study, at P11, in addition to VGluT1, Cadm1 partly co-localized with Synaptophysin, a pre-synaptic marker, and PSD-95, a post-synaptic marker, in the molecular layer (Figure S4). In a separate study, we found that Cadm1 also co-localized with GABBR2 on the dendrites of Purkinje cells during development (Fujita et al., submitted). Thus, Cadm1 may localize at the pre-synapse and post-synapse of the parallel fiber–Purkinje cells. The reduced immunoreactivity of Cadm1 on the dendrites of Purkinje cells in the *Foxp2*(R552H) KI mice could result from the decreased number of synapses. Foxp2 is essential for Purkinje cell development, while Cadm1 activity at parallel fiber–Purkinje cell synapses may be involved in mouse USV, and perhaps also in human spoken language. However, we note that loss of Cadm1 activity in other brain regions could also contribute to or even cause the vocalization phenotype, an important issue that future studies should address.

Cadm1 expression and Foxp2

The *CADM1* mutations H246N and Y251S have been identified in people with ASD who also had speech and language impairment [5]. In the current study, we found that *Cadm1* KO male mice (C57BL/6) had small cerebellums (Figure 1), impaired USV (Figure 2), and abnormal social and emotional behaviors, analogous to some behaviors associated with ASD [8].

ASD patients with mutations in the *CNTNAP2* gene also exhibit impaired speech and language [23]. A recent study showed that FOXP2 binds to the CAAATT motif in an intron of the human *CNTNAP2* gene, resulting in negative regulation of *CNTNAP2* expression; mutant FOXP2 (R553H) lacking DNA-binding activity resulted in increased *CNTNAP2* expression in *in vitro* experiments [11]. Human *CADM1* and mouse *Cadm1* have the same CAAATT binding motif for FOXP2 (accession no. NC_000011.9 for human *CADM1* and accession no. NC_000075.5 for mouse *Cadm1*). In contrast to CNTNAP2, we found here that Cadm1 mRNA levels were unchanged in the cerebellum of *Foxp2*(R552H) KI mice (Figure S1). Therefore, Foxp2 does not appear to regulate directly the expression of mouse *Cadm1* in the cerebellum. Thus, *Cadm1* and *CNTNAP2* exhibit different sensitivities to Foxp2 regulation, although they have the same CAAATT motif. This distinction may be attributable to different conditions in *in vitro* and *in vivo* experiments or to subtle variations in the binding motifs in the *Cadm1* and *CNTNAP2* genes; the nucleotide sequence of the repeated CAAATT motif, which is necessary for binding of dimerized Foxp2, may differ between the two genes.

In conclusion, *Cadm1* is not a target of the Foxp2 transcription factor, but Cadm1 activity at parallel fiber–Purkinje cell synapses may be necessary for USV function. Loss of Cadm1 activity at the synapse may be associated not only with USV impairment in mice but also with impaired speech and language communication skills in people with ASD.

Materials and Methods

Ethics statement

We followed the Fundamental Guidelines for Proper Conduct of Animal Experiments and Related Activities in Academic Research Institutions under the jurisdiction of the Ministry of Education, Culture, Sports, Science and Technology, and all of the protocols for animal handling and treatment were reviewed and approved by the Animal Care and Use Committee of Jichi University (approval numbers, H22-179, 10-179) and International University of Health and Welfare (approval numbers, D1008; 10118). Wild-type, *Cadm1* KO and *Foxp2*(R552H) KI mice [7,13] (male mice) were used for the experiments.

Ultrasonic vocalization

We mated *Cadm1* KO (129Sv) mice [7] with C57BL/6J strain mice for 10 generations and established a strain of *Cadm1* KO (C57BL/6J) mice. USVs of five *Cadm1* KO and five wild-type pups (P8) were assayed as described previously [13]. Briefly, each pup was separated from its mother and littermates, one at a time, placed in a shallow beaker in a soundproof chamber, and then positioned below a microphone connected to the UltraSound Gate 116 detector set (Avisoft Bioacoustics) to detect USVs of 40–100 kHz. Analysis began after the pup had been habituated to the chamber for 60 s. Sounds were recorded for 3 min.

Quantitative real-time PCR

Total RNA was prepared from a combined five pieces of cerebellum of wild-type and *Cadm1* KO and *Foxp2*(R552H) KI male mice (P10), respectively, using the RNeasy mini kit (Qiagen) according to the manufacturer's specifications. Complementary DNAs were synthesized from total RNA (1 μg) using reverse transcriptase (Invitrogen) as described previously [24]. Real-time PCR analysis was performed using the Applied Biosystems 7500 fast real-time PCR system (Applied Biosystems) with the TaqMan Gene Expression Assays (Applied Biosystems) based on published sequences for genes encoding the respective mouse Cadm1, Foxp2, and VIC-labeled mouse Gapd (VIC-labeled MGD probe; Applied Biosystems) as endogenous control. For each sample, the 20 μl total volume consisted of 10 μl TaqMan Fast Universal PCR Master Mix (2x; Applied Biosystems), 1 μl TaqMan Gene Expression Assays, and 5 μl of each first-strand cDNA sample. The real-time PCR fragments were amplified as follows: 1 cycle at

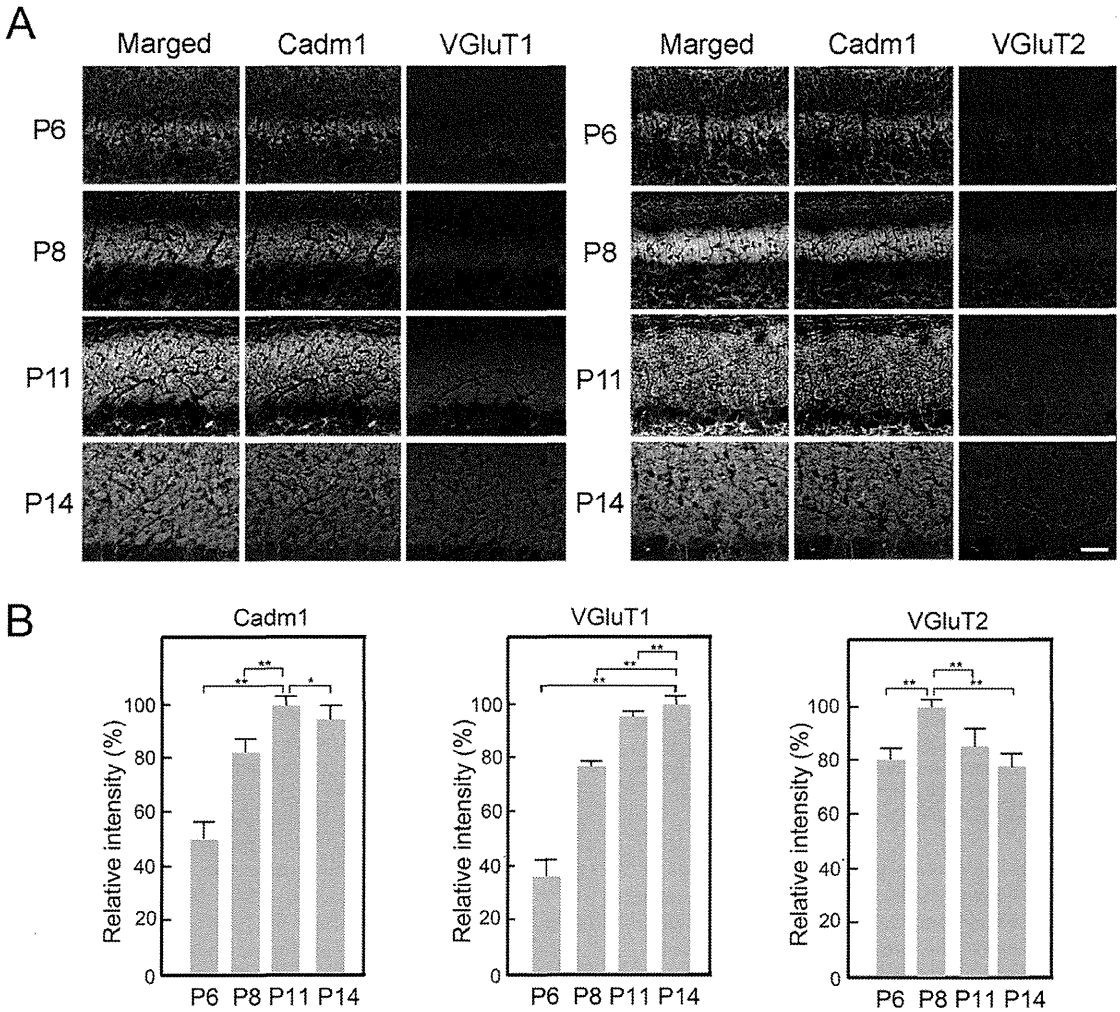

Figure 4. Developmental changes of Cadm1, VGluT1, and VGluT2 in wild-type pups. Alteration of the distribution of Cadm1, VGluT1, and VGluT2 was examined in the molecular layer of the developing cerebellum (P6–14). VGluT2 first appeared in the molecular layer in the early postnatal cerebellum (P6–8), in which Cadm1 co-localized with VGluT2, and then the level of VGluT2 decreased. VGluT1 increased in the later postnatal cerebellum (P11–14), in which Cadm1 co-localized with VGluT1. Green, Cadm1. Red, VGluT1 or VGluT2. Blue, Hoechst. Bar, 30 μm. Values are mean±standard error (SEM). Student's *t*-test (*$p<0.05$, **$p<0.01$). Pups: n = 3. Images: n = 8.
doi:10.1371/journal.pone.0030151.g004

95°C for 20 s, 60 cycles at 95°C for 3 s, and 60°C for 30 s. Results were analyzed using student's *t*-tests ($p<0.05$ was considered statistically significant).

Immunblot analysis

Five cerebellums each from wild-type and *Cadm1* KO mice, respectively, were combined and lysed in lysis buffer [50 mM Tris-HCl pH 8.0, 150 mM NaCl, 10% glycerol, 0.5% IGEPAL CA630, and protease inhibitors; complete mini (Roche Diagnostics)] at 4°C for 15 min, and then each extract was subjected to immunoblot analysis using mouse anti-Synaptophysin (Millipore), rabbit anti-VGluT1 (Synaptic Systems), rabbit anti-Foxp2 (Abcam), and mouse anti-Tubulin (Sigma). Immunoreactivity was visualized using alkaline phosphatase-conjugated anti-mouse or anti-rabbit IgG, Nitro blue tetrazolium, and 5-bromo-4-chloro-3-indolyl-1-phosphate (Roche Diagnostics). Data from three experiments were scanned and analyzed for quantification with Image J software (National Institutes of Health). Results compared with wild-type were analyzed using the student's *t*-test ($p<0.05$ was considered statistically significant).

Immunostaining

Wild-type, *Cadm1* KO, and *Foxp2*(R552H) KI mice cerebellums were fixed in 4% paraformaldehyde in phosphate buffered saline at 4°C overnight. Frozen sections (10 μm thick) were cut on a cryostat and immunostained with chicken anti-SynCAM1 (Cadm1; MBL), mouse anti-Calbindin (Sigma), rabbit anti-Calbindin (Sigma), mouse anti-Synaptophysin, rabbit anti-VGluT1, or rabbit anti-VGluT2 (Synaptic Systems). Alexa Fluor 488– and Alexa Fluor 568-conjugated secondary antibodies against mouse, rabbit, and goat IgGs were purchased from Molecular Probes. Nuclei were detected by Hoechst 33342 (Molecular Probes). The reactivity was viewed using a Leica SP5 confocal microscope (Leica Microsystems). At least three

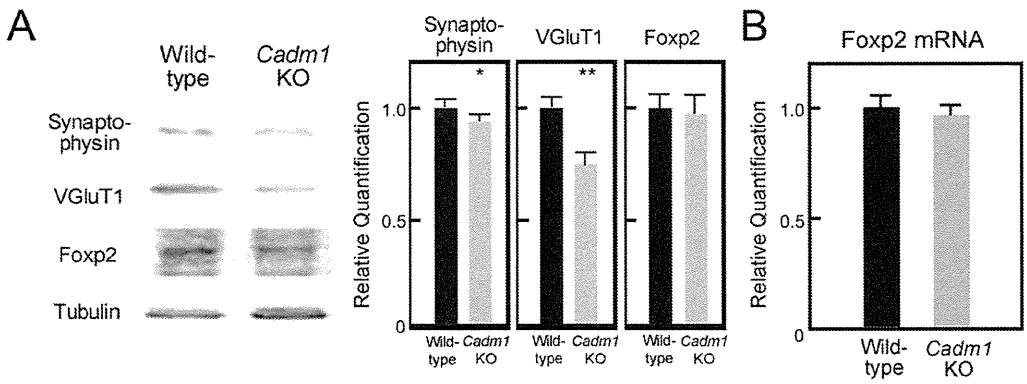

Figure 5. The influence of Cadm1 deficiency on the expression of synaptic proteins and Foxp2 in the cerebellum. (A) Immunoblot analysis of the influence of the deficiency in the cerebellums of *Cadm1* KO and wild-type pups (P10). An example of the typical immunoblotting results is shown. Values are mean±standard error (SEM). Student's *t*-test (*$p<0.05$, **$p<0.01$). Pups: n = 5. All experiments were performed three times. (B) RT-PCR analysis of the influence of the Cadm1 deficiency on the expression of *Foxp2* in the cerebellum of wild-type and *Cadm1* KO pups (P10). Values are mean±standard error (SEM). Pups: n = 5. All experiments were performed three times. A comparison showed no significant difference (Student's *t*-test; $p<0.05$).
doi:10.1371/journal.pone.0030151.g005

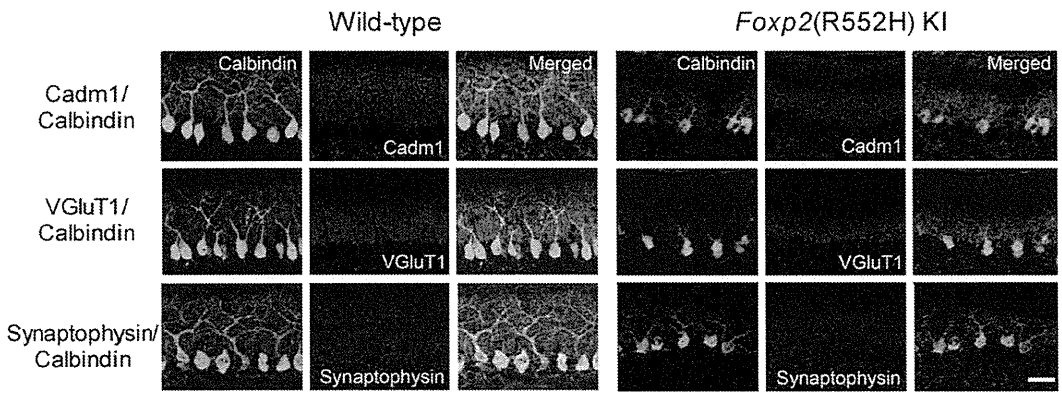

Figure 6. Altered distribution of Cadm1 in the molecular layer of wild-type and *Foxp2*(R552H) KI mice (P11). Cadm1 preferentially distributed in the apical–distal dendritic portion in the molecular layer. The immunoreactivity of Cadm1 as well as that of Synaptophysin and VGluT1, pre-synaptic markers, was decreased in the molecular layer of the *Foxp2*(R552H) KI mice. Green, Calbindin. Red, Cadm1, VGluT1, Synaptophysin. Blue, Hoechst. Bar, 30 μm.
doi:10.1371/journal.pone.0030151.g006

animals per genotype were examined, and experiments were repeated three times. Quantification of staining intensities was done using LAS AF software (Leica Microsystems). The mean pixel value in the area of interest and in the same size area of the background was calculated. The background level was subtracted from the value found in the area of interest (in the molecular layer). Reported intensities were normalized to control, and the Student's *t*-test was performed for statistical analysis.

Supporting Information

Figure S1 Alteration of Purkinje cells in cerebellum of wild-type and *Foxp2*(R552H) knock-in (*Foxp2* KI) mice, wild-type, and *Cadm1* knockout (*Cadm1* KO) (P11). The immunoreactivity was performed using mouse anti-Calbindin. Bar, 20 μm.
(TIF)

Figure S2 Altered distribution of the Cadm1 of wild-type and *Foxp2*(R552H) KI mice (P11). Values are mean± standard error (SEM). Student's *t*-test (**$p<0.01$). Pups: n = 3. Images: n = 10.
(TIF)

Figure S3 RT-PCR analysis of the expression of *Cadm1* in the cerebellum of wild-type and *Foxp2*(R552H) KI mice (P10). Values are mean±standard error (SEM). Pups: n = 5. All experiments were performed three times. A comparison showed no significant difference (Student's *t*-test; $p<0.05$).
(TIF)

Figure S4 The immunoreactivity (p11) of Synaptophysin (pre-synaptic marker) and PSD-95 (post-synaptic marker). Green, Cadm1. Red, Synaptophysin or PSD-95 (Cell Signaling Technology). Blue, Hoechst. Bar, 30 μm.
(TIF)

Author Contributions

Conceived and designed the experiments: TM MYM BI. Performed the experiments: EF YT. Analyzed the data: EF TM. Contributed reagents/materials/analysis tools: EF TM. Wrote the paper: EF BI TM.

References

1. Biederer T, Sara Y, Mozhayeva M, Atasoy D, Liu X, et al. (2002) SynCAM, a synaptic adhesion molecule that drives synapse assembly. Science 297: 1525–1531.
2. Fujita E, Soyama A, Momoi T (2003) RA175, which is the mouse ortholog of TSLC1, a tumor suppressor gene in human lung cancer, is a cell adhesion molecule. Exp Cell Res 287: 57–66.
3. Jamain S, Quach H, Betancur C, Råstam M, Colineaux C, et al. (2003) Mutations of the X-linked genes encoding neuroligins NLGN3 and NLGN4 are associated with autism. Nat Genet 34: 27–29.
4. Bakkaloglu B, O'Roak BJ, Louvi A, Gupta AR, Abelson JF, et al. (2008) Molecular cytogenetic analysis and resequencing of contactin associated protein-like 2 in autism spectrum disorders. Am J Hum Genet 82: 165–173.
5. Zhiling Y, Fujita E, Tanabe Y, Yamagata T, Momoi T, et al. (2008) Mutations in the gene encoding CADM1 are associated with autism spectrum disorder. Biochem Biophys Res Commun 377: 926–929.
6. Fujita E, Dai H, Tanabe Y, Zhiling Y, Yamagata T, et al. (2010) Autism Spectrum Disorder is related to endoplasmic reticulum stress induced by mutations in the synaptic cell adhesion molecule, CADM1. Cell death disease 1: e47.
7. Fujita E, Kouroku Y, Ozeki S, Tanabe Y, Toyama Y, et al. (2006) Oligo-astheno-teratozoospermia in mice lacking RA175/TSLC1/SynCAM/IGSF4A, a cell adhesion molecule in the immunoglobulin superfamily. Mol Cell Biol 26: 718–726.
8. Takayanagi Y, Fujita E, Yu Z, Yamagata T, Momoi MY, et al. (2010) Impairment of social and emotional behaviors in Cadm1-knockout mice. Biochem Biophys Res Commun 396: 703–708.
9. Lai CS, Fisher SE, Hurst JA, Vargha-Khadem F, Monaco AP (2001) A forkhead-domain gene is mutated in a severe speech and language disorder. Nature 413: 519–523.
10. Li S, Weidenfeld J, Morrisey EE (2004) Transcriptional and DNA binding activity of the Foxp1/2/4 family is modulated by heterotypic and homotypic protein interactions. Mol Cell Biol 24: 809–822.
11. Vernes SC, Newbury DF, Abrahams BS, Winchester L, Nicod J, et al. (2008) A functional genetic link between distinct developmental language disorders. N Engl J Med 359: 2337–2345.
12. Branchi I, Santucci D, Alleva E (2001) Ultrasonic vocalisation emitted by infant rodents: a tool for assessment of neurobehavioural development. Behav Brain Res 125: 49–56.
13. Fujita E, Tanabe Y, Shiota A, Ueda M, Suwa K, et al. (2008) Ultrasonic vocalization impairment of Foxp2 (R552H) knockin mice related to speech-language disorder and abnormality of Purkinje cells. Proc Natl Acad Sci USA 105: 3117–3122.
14. Shu W, Cho JY, Jiang Y, Zhang M, Weisz D, et al. (2005) Altered ultrasonic vocalization in mice with a disruption in the Foxp2 gene. Proc Natl Acad Sci USA 102: 9643–9648.
15. Ritvo ER, Freeman BJ, Scheibel AB, Duong T, Robinson H, et al. (1986) Lower Purkinje cell counts in the cerebella of four autistic subjects: initial findings of the UCLA-NSAC Autopsy Research Report. Am J Psychiatry 143: 862–866.
16. Urase K, Soyama A, Fujita E, Momoi T (2001) Expression of RA175 mRNA, a new member of the immunoglobulin superfamily, in developing mouse brain. Neuroreport 12: 3217–3221.
17. Fujita E, Urase K, Soyama A, Kouroku Y, Momoi T (2005) Distribution of RA175/TSLC1/SynCAM, a member of the immunoglobulin superfamily, in the developing nervous system. Brain Res Dev Brain Res 154: 199–209.
18. Miyazaki T, Fukaya M, Shimizu H, Watanabe M (2003) Subtype switching of vesicular glutamate transporters at parallel fibre-Purkinje cell synapses in developing mouse cerebellum. Eur J Neurosci 17: 2563–2572.
19. Boulland JL, Qureshi T, Seal RP, Rafiki A, Gundersen V, et al. (2004) Expression of the vesicular glutamate transporters during development indicates the widespread corelease of multiple neurotransmitters. J Comp Neurol 480: 264–280.
20. Xue G, Dong Q, Jin Z, Chen C (2004) Mapping of verbal working memory in nonfluent Chinese-English bilinguals with functional MRI. Neuroimage 22: 1–10.
21. Dietrich S, Hertrich I, Alter K, Ischebeck A, Ackermann H (2008) Understanding the emotional expression of verbal interjections: a functional MRI study. Neuroreport 19: 1751–1755.
22. Robbins EM, Krupp AJ, Perez de Arce K, Ghosh AK, Fogel AI, et al. (2010) SynCAM 1 adhesion dynamically regulates synapse number and impacts plasticity and learning. Neuron 68: 894–906.
23. Newbury DF, Monaco AP (2010) Genetic advances in the study of speech and language disorders. Neuron 68: 309–320.
24. Fujita E, Tanabe Y, Hirose T, Aurrand-Lions M, Kasahara T, et al. (2007) Loss of partitioning-defective-3/isotype-specific interacting protein (par-3/ASIP) in the elongating spermatid of RA175 (IGSF4A/SynCAM)-deficient mice. Am J Pathol 171: 1800–1810.

Neuroscience Letters 506 (2012) 277–280

Contents lists available at SciVerse ScienceDirect

Neuroscience Letters

journal homepage: www.elsevier.com/locate/neulet

Cntnap2 expression in the cerebellum of *Foxp2*(R552H) mice, with a mutation related to speech-language disorder

Eriko Fujita[a,b], Yuko Tanabe[a], Mariko Y. Momoi[b], Takashi Momoi[a,*]

[a] *Center for Medical Science, International University of Health and Welfare, 2600-1, Kitakanemaru, Ohtawara, Tochigi, Japan*
[b] *Department of Pediatrics, Jichi Medical University, 3311-1 Yakushiji, Shimotsukeshi, Tochigi 329-0498, Japan*

ARTICLE INFO

Article history:
Received 23 July 2011
Received in revised form 5 November 2011
Accepted 13 November 2011

Keywords:
Foxp2
CtBP
Speech-language
Cntnap2

ABSTRACT

Foxp2(R552H) knock-in (KI) mice carrying a mutation related to human speech-language disorder exhibit impaired ultrasonic vocalization and poor Purkinje cell development. Foxp2 is a forkhead domain-containing transcriptional repressor that associates with its co-repressor CtBP; Foxp2(R552H) displays reduced DNA binding activity. A genetic connection between FOXP2 and *CNTNAP2* has been demonstrated *in vitro*, but not *in vivo*. Here we show that Cntnap2 mRNA levels significantly increased in the cerebellum of *Foxp2*(R552H) KI pups, although the cerebellar population of Foxp2-positive Purkinje cells was very small. Furthermore, Cntnap2 immunofluorescence did not decrease in the poorly developed Purkinje cells of *Foxp2*(R552H) KI pups, although synaptophysin immunofluorescence decreased. Cntnap2 and CtBP were ubiquitously expressed, while Foxp2 co-localized with CtBP only in Purkinje cells. Taken together, these observations suggest that Foxp2 may regulate ultrasonic vocalization by associating with CtBP in Purkinje cells; *Cntnap2* may be a target of this co-repressor.

© 2011 Elsevier Ireland Ltd. All rights reserved.

1. Introduction

Autism spectrum disorder (ASD) is one of the most heritable neurodevelopmental disorders [22]. Mutations in the genes encoding contactin-associated protein 2 (CNTNAP2 and Caspr2) have been identified in patients with ASD and impaired speech-language [2,3]. On the other hand, *FOXP2*, a forkhead box-containing gene, is the causative gene of speech-language disorder [17]; the missense mutation FOXP2 (R553H) co-segregates with members of the KE family affected with speech-language disorder.

Cntnap2 is an adhesion molecule required for the formation of axoglial paranodal junctions surrounding the nodes of Ranvier in myelinated axons [21,23]. In the human brain, CNTNAP2 is also expressed in the circuits important for language development [2]. Cntnap2 is localized to the synaptic plasma membrane fraction [3] and to membrane traffic vesicles [4,20]. The C-terminal region of Cntnap2 contains the PDZ binding domain EYFI [14], which is similar to that of Cadm1, a synaptic adhesion molecule related to ASD [11,19,26]. Cntnap2 associates in *cis* with the contactin family, the glycosyl-phosphatidyl inositol-anchored neural cell adhesion molecule contactin/F3, TAG-1, NB-1, and NB-2, molecules required for the transport of Cntnap2 to the cell surface [9]. Cntnap2 also acts as a negative regulator of neurite outgrowth [8].

The relationship between speech-language disorder and ASD is not clear, although impaired social communication, including speech-language, is one of the phenotypes of ASD patients. FOXP2 has DNA-binding activity and exhibits repressor activity via its interaction with co-repressors such as C-terminal binding protein (CtBP) [18]. A genetic connection between FOXP2 and *CNTNAP2* has been shown *in vitro* [25]; FOXP2 binds the CAAATT motif in an intron of *CNTNAP2* and negatively regulates the expression of CNTNAP2 mRNA, but FOXP2(R553H) does not.

Infant rodents emit ultrasonic vocalizations (USVs), whistle-like sounds of frequencies between 40 and 100 kHz, that play an important communicative role in mother–offspring interactions when the pups are isolated from their mother and littermates [5]. *Foxp2* knock-out (KO) pups and knock-in (KI) pups harboring the *Foxp2*(R552H) mutation that corresponds to the human *FOXP2*(R553H) mutation exhibit severe USV impairment, suggesting that human speech and mouse USVs have a common molecular basis in the brain [15,24]. *Foxp2*(R552H) KI mice also display poor Purkinje cell development in the cerebellum [15]. Microarray analysis of the cerebellar gene expression of *Foxp2*(R552H) KI pups (P10) suggests that Foxp2 regulates USV-related gene expression in Purkinje cells.

To provide additional insight into the relationship between impairment of speech-language and ASD, we examined co-localization of CtBP and Foxp2 as well as Cntnap2 expression in the cerebellum of *Foxp2*(R552H) KI mice with impaired USV. Our

Abbreviations: Cntnap2, contactin-associated protein 2; CtBP, C-terminal binding protein; USV, ultrasonic vocalization; ASD, autism spectrum disorder.

* Corresponding author. Tel.: +81 287 24 3162; fax: +81 287 24 3162.
E-mail address: momoi@iuhw.ac.jp (T. Momoi).

0304-3940/$ – see front matter © 2011 Elsevier Ireland Ltd. All rights reserved.
doi:10.1016/j.neulet.2011.11.022

observations demonstrate the *in vivo* genetic connection between Foxp2 and *Cntnap2*.

2. Materials and methods

We followed the fundamental guidelines for proper conduct of animal experiment and related activities in Academic Research Institutions under the jurisdiction of the Ministry of Education, Culture, Sports, Science and Technology, and all of the protocols for animal handling and treatment were reviewed and approved by the Animal Care and Use Committee of Jichi University (approval numbers, H22-179; 10-179) and International University of Health and Welfare (approval numbers, D1008; 10118). Wild-type and *Foxp2*(R552H) KI mice (129/sv) [15] (male mice) were used for experiments.

Mouse brains were fixed in 4% paraformaldehyde in phosphate buffered saline (PBS) at 4 °C overnight. Frozen sections (10 μm thick) were cut on a cryostat and immunostained with mouse anti-calbindin (Sigma), rabbit anti-calbindin (Sigma), mouse anti-synaptophysin (Sigma), mouse anti-CTBP (Santa Cruz Biotech.), rabbit anti-caspr2 (Cntnap2; Abcam), and rabbit anti-Foxp2 (Abcam). Alexa Fluor 488 and Alexa Fluor 568 conjugated secondary antibodies against mouse and rabbit IgG were purchased from Molecular Probes. Nuclei were detected by Hoechst 33342 (Molecular Probes). The reactivity was viewed using a Leica AF6000 immunofluorescence microscope or a Leica SP5 confocal microscope (Leica Microsystems). At least three different animals per genotype and experiments were repeated three times.

Total RNA was prepared from brains of wild-type and *Cadm1* KO [13] and *Foxp2*(R552H) KI male mice [15] by RNeasy mini kit (Qiagen) according to the manufacturer's specifications. Complementary DNAs were synthesized from total RNA (1 μg) using reverse transcriptase (Invitrogen) as described previously [12]. Quantitative real-time (RT) PCR analysis was performed by Applied Biosystems 7500 fast real-time PCR system (Applied Biosystems) using the TaqMan Gene Expression Assays (Applied Biosystems) based on published sequences for genes encoding the respective mouse *Cntnap2*, and VIC-labeled mouse Gapd (VIC-labeled MGD probe; Applied Biosystems) as endogenous control. For each sample, the 20 μl total volume consisted of 10 μl TaqMan Fast Universal PCR Master Mix (2×; Applied Biosystems), 1 μl TaqMan Gene Expression Assays, and 5 μl of each first-strand cDNA sample. The real-time PCR fragments were amplified as follows: 1 cycle at 95 °C for 20 s, 60 cycles at 95 °C for 3 s and 60 °C for 30 s. Results were analysed by Student's *t*-test ($p < 0.05$ was considered statistically significant).

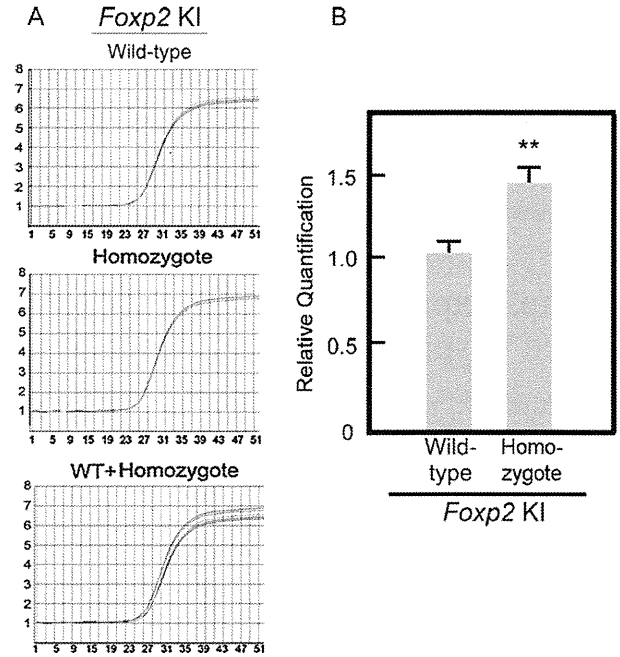

Fig. 1. Increased expression of Cntnap2 in the cerebellum of *Foxp2*(R552H) KI mice (P10). Quantitative real-time PCR analysis of the expression of Cntnap2 mRNA in the cerebellum of *Foxp2*(R552H) KI mice (A and B). The expression of Cntnap2 mRNA in *Foxp2*(R552H) KI mice was compared with that in wild-type mice. Values are mean ± SEM for at least three independent determinations. Student's *t*-test (**$p < 0.01$).

3. Results

We quantitatively measured the level of Cntnap2 mRNA in the cerebella of wild-type and *Foxp2*(R552H) KI pups (P10). The level of Cntnap2 mRNA increased 1.6-fold ($p < 0.05$) in the cerebellum of *Foxp2*(R552H) KI mice (Fig. 1A and B). However, the mRNA levels of other genes, including *Cadm1*, were unchanged (Supplementary Fig. S1). Thus, the expression of *Cntnap2* appears to be under the control of Foxp2 in the cerebellum.

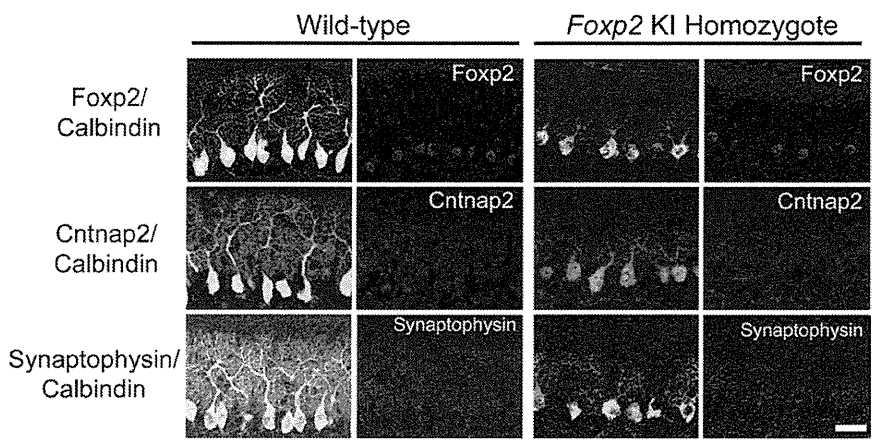

Fig. 2. Cntnap2 localization in the cerebellum of *Foxp2*(R552H) KI pups. Cntnap2 distribution was examined in the cerebellum of wild-type and *Foxp2*(R552H) KI pups (P10) by immunostaining. The Cntnap2 intensity preferentially distributed in the proximal dendritic portion. In contrast with synaptophysin, intensity of Cntnap2 immunoreactivity was not decreased in the *Foxp2*(R552H) KI pups. Green; calbindin. Red; Foxp2, Cntnap2 or synaptophysin. Blue; Hoechst. Bar indicates 30 μm.

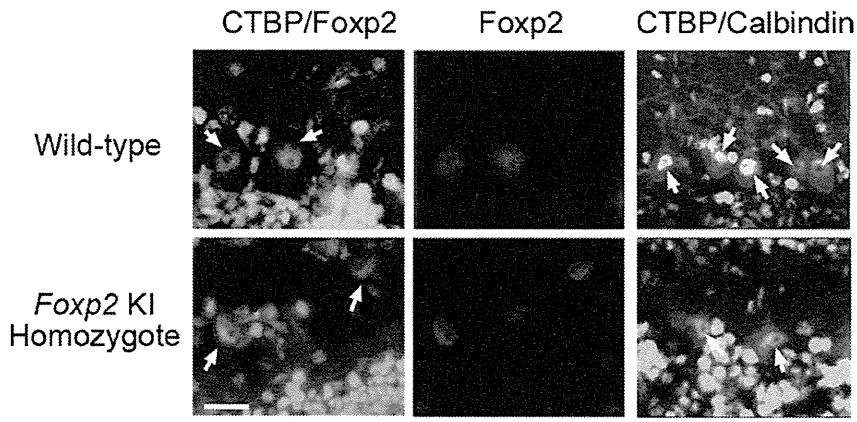

Fig. 3. Localization and distribution of CtBP in the cerebellum of wild-type and *Foxp2*(R552H) KI mice (P10). The CtBP co-localized with Foxp2 (left panel). The CtBP localized both in the Purkinje cells and granular cells (right panel). As Foxp2 localized in the nuclei of Purkinje cells (see Fig. 2), the CtBP co-localized with Foxp2 in the nuclei of Purkinje cells. Green; CTBP. Red; Foxp2 or calbindin. Blue; Hoechst. Bar indicates 30 μm.

To elucidate the role of Cntnap2 in USV, we examined Cntnap2 localization in the cerebella of wild-type and *Foxp2*(R552H) KI mice. Cntnap2 immunoreactivity was preferentially located in the soma and proximal dendritic portion of Purkinje cells, as well as in the granular cells of the wild-type P10 pups (Fig. 2). *Foxp2*(R552H) KI pups exhibited poor development of Purkinje cell dendrites with reduced synaptophysin immunoreactivity [15]. In contrast, the intensity of Cntnap2 immunofluorescence was apparently unchanged (Fig. 2). However, given the poor development and decreased number (20% reduction) of Purkinje cells in the *Foxp2*(R552H) KI pups, the intensity of Cntnap2 immunofluorescence seems to be relatively increased in the Purkinje cells.

Foxp2 associates with its co-repressor CtBP and acts as a transcriptional repressor [18]. In the cerebellum, CtBP localized to the nuclei of granular cells and Purkinje cells (Fig. 3, right), while Foxp2 localized to the nuclei of Purkinje cells but not granular cells (Fig. 2). CtBP co-localized with Foxp2 and Foxp2(R552H) in the Purkinje cells of wild-type and *Foxp2*(R552H) KI mice, respectively (Fig. 3, left).

4. Discussion

Foxp2(R552H) KI mice exhibit abnormal cerebellar development and poor dendrite development [15]. In addition, the selective expression of FOXP2 in the Purkinje cells of *Foxp2*(R552H) KI mice partially improves their USVs (unpublished observation), suggesting that Purkinje cells are an essential component of the Foxp2-mediated USV network. We observed a statistically significant increase in Cntnap2 mRNA levels in *Foxp2*(R552H) KI mice. Expression of Cntnap2 and its co-repressor CtBP was ubiquitous in granular cells and Purkinje cells, but Foxp2 expression was restricted to the Purkinje cells. Given the ratio of granular cells to Purkinje cells in the cerebellum, Cntnap2 mRNA must be up-regulated in the Purkinje cells of the *Foxp2*(R552H) KI mice more than 1.6 fold. Thus, our observations suggest that Cntnap2 is a Foxp2 target in Purkinje cells, and that the Foxp2 and CtBP complex acts as a transcriptional repressor.

The apparently unchanged intensity of Cntnap2 immunofluorescence in *Foxp2*(R552H) KI mice, which display poor Purkinje cell dendrite development and decreased synaptophysin immunofluorescence, suggests that Cntnap2 expression is relatively increased in the decreased number of synapses on the dendrites. Cntnap2 must be up-regulated and degraded, whereas synaptophysin may not be up-regulated but is degraded.

Human speech and mouse USVs have a common molecular basis in the brain that is mediated by Foxp2 [15,24], and the cerebellum is related to the network engaged in the production of spoken human language [1,6]. Functional magnetic resonance imaging has suggested the existence of two cerebrocerebellar networks for human verbal working memory; cerebellar abnormality with Purkinje cell loss has been observed in several autopsy samples from ASD patients [10]. A *Cntnap2* mutation occurs in ASD patients with speech-language disorder [2,3], suggesting that Cntnap2 is an essential factor for speech-language. However, Cntnap2 is relatively up-regulated in the Purkinje cells of *Foxp2*(R552H) KI pups (Fig. 1) with impaired USV. Cntnap2 is a negative regulator of neurite outgrowth [8], suggesting that Cntnap2 may be a negative regulator in the network involved in Foxp2-mediated USV and/or speech-language. However, it is presently unclear why Cntnap2-mediated negative regulation is necessary for Foxp2-mediated USV. This unresolved question will be an important issue for future study; USV and speech-language function may be regulated by a dual positive and negative synaptic system.

Cntnap2 may cooperate or compete with synaptic adhesion molecules, including Cadm1, in Foxp2-mediated USV. Mutations in *CADM1* and *NLGN-3* occur in ASD patients [7,26]. *Cadm1* KO, as well as *Nlgn-3*- and *Nlgn-4*-deficient mice, exhibit impaired USV [16], and Cadm1 localizes to the molecular layer of the dendritic arbor of Purkinje cells, with reduced distribution in *Foxp2*(R552H) KI pups (Fujita et al., submitted). Cntnap2 localized not only to the proximal dendrites, but also to the soma of Purkinje cells (Fig. 2) and to membrane traffic vesicles [4,20], indicating that Cntnap2 is involved in the membrane trafficking of synaptic molecules to the synapse. Since the cytoplasmic tail of Cntnap2 carries a PDZ binding motif identical to the one in Cadm1, and since its *cis*-binding partners are members of the contactin family of the immunoglobulin superfamily, it may be possible that the contactin-2(TAG-1)-Cntnap2 complex and Cadm1 cooperatively or competitively participate in speech-language and USV activity in the molecular layer.

In conclusion, *Cntanp2* expression is repressed by Foxp2 in Purkinje cells. Cntnap2 may cooperate or compete with synaptic molecules such as Cadm1 in Foxp2-mediated USV and speech-language.

Conflict of interest

The authors declare no conflict of interest.

Acknowledgements

This work was supported by Grants-in-Aid for Scientific Research (KAKENHI) of the Ministry of Education, Culture, Sports, Science and Technology, Japan (21200011, 21700377); Grants-in-Aid for Health Labour Scientific Research of the Ministry of the Health, Labour and Welfare, Japan (10103243).

Appendix A. Supplementary data

Supplementary data associated with this article can be found, in the online version, at doi:10.1016/j.neulet.2011.11.022.

References

[1] H. Ackermann, Cerebellar contributions to speech production and speech perception: psycholinguistic and neurobiological perspectives, Trends Neurosci. 31 (2008) 265–272.
[2] M. Alarcon, B.S. Abrahams, J.L. Stone, J.A. Duvall, J.V. Perederiy, J.M. Bomar, J. Sebat, M. Wigler, C.L. Martin, D.H. Ledbetter, S.F. Nelson, R.M. Cantor, D.H. Geschwind, Linkage, association, and gene-expression analyses identify CNTNAP2 as an autism-susceptibility gene, Am. J. Hum. Genet. 82 (2008) 150–159.
[3] B. Bakkaloglu, B.J. O'Roak, A. Louvi, A.R. Gupta, J.F. Abelson, T.M. Morgan, K. Chawarska, A. Klin, A.G. Ercan-Sencice, A.A. Stillman, G. Tanriover, B.S. Abrahams, J.A. Duvall, E.M. Robbins, D.H. Geschwind, T. Biederer, M. Gunel, R.P. Lifton, M.W. State, Molecular cytogenetic analysis and resequencing of contactin associated protein-like 2 in autism spectrum disorders, Am. J. Hum. Genet. 82 (2008) 165–173.
[4] C. Bel, K. Oguievetskaia, C. Pitaval, L. Goutebroze, C. Faivre-Sarrailh, Axonal targeting of Caspr2 in hippocampal neurons via selective somatodendritic endocytosis, J. Cell Sci. 122 (2009) 3403–3413.
[5] I. Branchi, D. Santucci, E. Alleva, Ultrasonic vocalisation emitted by infant rodents: a tool for assessment of neurobehavioural development, Behav. Brain Res. 125 (2001) 49–56.
[6] S.H. Chen, J.E. Desmond, Cerebrocerebellar networks during articulatory rehearsal and verbal working memory tasks, Neuroimage 24 (2005) 332–338.
[7] D. Comoletti, A. De Jaco, L.L. Jennings, R.E. Flynn, G. Gaietta, I. Tsigelny, M.H. Ellisman, P. Taylor, The Arg451Cys-neuroligin-3 mutation associated with autism reveals a defect in protein processing, J. Neurosci. 24 (2004) 4889–4893.
[8] V. Devanathan, I. Jakovcevski, A. Santuccione, S. Li, H.J. Lee, E. Peles, I. Leshchyns'ka, V. Sytnyk, M. Schachner, Cellular form of prion protein inhibits Reelin-mediated shedding of Caspr from the neuronal cell surface to potentiate Caspr-mediated inhibition of neurite outgrowth, J. Neurosci. 30 (2010) 9292–9305.
[9] C. Faivre-Sarrailh, F. Gauthier, N. Denisenko-Nehrbass, A. Le Bivic, G. Rougon, J.A. Girault, The glycosylphosphatidyl inositol-anchored adhesion molecule F3/contactin is required for surface transport of paranodin/contactin-associated protein (caspr), J. Cell Biol. 149 (2000) 491–502.
[10] S.H. Fatemi, A.R. Halt, G. Realmuto, J. Earle, D.A. Kist, P. Thuras, A. Merz, Purkinje cell size is reduced in cerebellum of patients with autism, Cell Mol. Neurobiol. 22 (2002) 171–175.
[11] E. Fujita, H. Dai, Y. Tanabe, Y. Zhiling, T. Yamagata, T. Miyakaw, M. Tanokura, M.Y. Momoi, T. Momoi, Autism spectrum disorder is related to endoplasmic reticulum stress induced by mutations in the synaptic cell adhesion molecule, CADM1, Cell Death Dis. 1 (2010) e47.
[12] E. Fujita, Y. Khoroku, K. Urase, T. Tsukahara, M.Y. Momoi, H. Kumagai, T. Takemura, T. Kuroki, T. Momoi, Involvement of Sonic hedgehog in the cell growth of LK-2 cells, human lung squamous carcinoma cells, Biochem. Biophys. Res. Commun. 238 (1997) 658–664.
[13] E. Fujita, Y. Kouroku, S. Ozeki, Y. Tanabe, Y. Toyama, M. Maekawa, N. Kojima, H. Senoo, K. Toshimori, T. Momoi, Oligo-astheno-teratozoospermia in mice lacking RA175/TSLC1/SynCAM/IGSF4A, a cell adhesion molecule in the immunoglobulin superfamily, Mol. Cell. Biol. 26 (2) (2006 Jan) 718–726.
[14] E. Fujita, A. Soyama, T. Momoi, RA175, which is the mouse ortholog of TSLC1, a tumor suppressor gene in human lung cancer, is a cell adhesion molecule, Exp. Cell Res. 287 (2003) 57–66.
[15] E. Fujita, Y. Tanabe, A. Shiota, M. Ueda, K. Suwa, M.Y. Momoi, T. Momoi, Ultrasonic vocalization impairment of Foxp2 (R552H) knockin mice related to speech-language disorder and abnormality of Purkinje cells, Proc. Natl. Acad. Sci. U.S.A. 105 (2008) 3117–3122.
[16] S. Jamain, K. Radyushkin, K. Hammerschmidt, S. Granon, S. Boretius, F. Varoqueaux, N. Ramanantsoa, J. Gallego, A. Ronnenberg, D. Winter, J. Frahm, J. Fischer, T. Bourgeron, H. Ehrenreich, N. Brose, Reduced social interaction and ultrasonic communication in a mouse model of monogenic heritable autism, Proc. Natl. Acad. Sci. U.S.A. 105 (2008) 1705–1710.
[17] C.S. Lai, S.E. Fisher, J.A. Hurst, F. Vargha-Khadem, A.P. Monaco, A forkhead-domain gene is mutated in a severe speech and language disorder, Nature 413 (2001) 519–523.
[18] S. Li, J. Weidenfeld, E.E. Morrisey, Transcriptional and DNA binding activity of the Foxp1/2/4 family is modulated by heterotypic and homotypic protein interactions, Mol. Cell. Biol. 24 (2004) 809–822.
[19] T. Momoi, E. Fujita, H. Senoo, M. Momoi, Genetic factors and epigenetic factors for autism: endoplasmic reticulum stress and impaired synaptic function, Cell Biol. Int. 34 (2009) 13–19.
[20] S. Oiso, Y. Takeda, T. Futagawa, T. Miura, S. Kuchiiwa, K. Nishida, R. Ikeda, H. Kariyazono, K. Watanabe, K. Yamada, Contactin-associated protein (Caspr) 2 interacts with carboxypeptidase E in the CNS, J. Neurochem. 109 (2009) 158–167.
[21] E. Peles, J.L. Salzer, Molecular domains of myelinated axons, Curr. Opin. Neurobiol. 10 (2000) 558–565.
[22] J. Pickett, E. London, The neuropathology of autism, J. Neuropathol. Exp. Neurol. 64 (2005) 925–935.
[23] S. Poliak, L. Gollan, R. Martinez, A. Custer, S. Einheber, J.L. Salzer, J.S. Trimmer, P. Shrager, E. Peles, Caspr2, a new member of the neurexin superfamily, is localized at the juxtaparanodes of myelinated axons and associates with K+ channels, Neuron 24 (1999) 1037–1047.
[24] W. Shu, J.Y. Cho, Y. Jiang, M. Zhang, D. Weisz, G.A. Elder, J. Schmeidler, R. De Gasperi, M.A. Sosa, D. Rabidou, A.C. Santucci, D. Perl, E. Morrisey, J.D. Buxbaum, Altered ultrasonic vocalization in mice with a disruption in the Foxp2 gene, Proc. Natl. Acad. Sci. U.S.A. 102 (2005) 9643–9648.
[25] S.C. Vernes, D.F. Newbury, B.S. Abrahams, L. Winchester, J. Nicod, M. Groszer, M. Alarcón, P.L. Oliver, K.E. Davies, D.H. Geschwind, A.P. Monaco, S.E. Fisher, A functional genetic link between distinct developmental language disorders, N. Engl. J. Med. 359 (2008) 2337–2345.
[26] Y. Zhiling, E. Fujita, Y. Tanabe, T. Yamagata, T. Momoi, M.Y. Momoi, Mutations in the gene encoding CADM1 are associated with autism spectrum disorder, Biochem. Biophys. Res. Commun. 377 (2008) 926–929.

First International Journal of Andrology
ANDROLOGIA

ORIGINAL ARTICLE

Localisation of RA175 (Cadm1), a cell adhesion molecule of the immunoglobulin superfamily, in the mouse testis, and analysis of male infertility in the RA175-deficient mouse

M. Maekawa[1], C. Ito[1], Y. Toyama[1], F. Suzuki-Toyota[1], E. Fujita[2], T. Momoi[2] & K. Toshimori[1]

1 Department of Anatomy and Developmental Biology, Graduate School of Medicine, Chiba University, Chiba, Japan;
2 Division of Differentiation and Development, Department of Inherited Metabolic Disorder, National Institute of Neuroscience, Tokyo, Japan

Keywords
Cadm1—immunoglobulin superfamily—infertility—spermatogenesis—testis

Correspondence
M. Maekawa, Department of Anatomy and Developmental Biology, Graduate School of Medicine, Chiba University, Chiba 260-8670, Japan.
Tel.: +81 43 226 2020;
Fax: +81 43 226 2021;
E-mail: mmaekawa@faculty.chiba-u.jp

Accepted: December 07, 2009

doi: 10.1111/j.1439-0272.2010.01049.x

Summary

RA175, a member of the immunoglobulin superfamily, plays an important role in cell adhesion, and *RA175* gene-deficient mice ($RA175^{-/-}$) show oligoasthenoteratozoospermia. To understand the function of RA175, location in the testis and the morphological features of its spermatogenic cells in $RA175^{-/-}$ mice were investigated. Immunohistochemical studies revealed that RA175 immunoreactivity was observed on the cell surface of the spermatogenic cells at specific stages. A strong reaction was detected from type A spermatogonia to pachytene spermatocytes at stage IV and from step 6 to step 16 spermatids during spermatogenesis. From pachytene spermatocytes at stage VI to step 4 spermatids, the reaction was not detected by the enzyme-labelled antibody method and was faintly detected by the indirect immunofluorescence method. Abnormal vacuoles in the seminiferous epithelium, showing exfoliation of germ cells, and ultrastructural abnormality of the elongate spermatids were revealed in the $RA175^{-/-}$ testes. Other members of the immunoglobulin superfamily such as basigin, nectin-2 and nectin-3, which have an important role in spermatogenesis, were immunohistochemically detected in the $RA175^{-/-}$ testis. These observations indicate a unique expression pattern of RA175 in the testis and provide clues regarding the mechanism of male infertility in the testis.

Introduction

Immunoglobulin superfamily (IgSF) molecules serve as cell adhesion receptors, and are implicated in diverse cellular phenomena such as cell shape and polarisation, cytoskeletal organisation, cell motility, proliferation, survival and differentiation (Holness & Simmons, 1994; Hynes, 1999). It is known that the IgSF members such as basigin and nectins are expressed in the testis and have a crucial function in spermatogenesis (Toshimori *et al.*, 2006). For example, basigin (CD147/EMMPRIN, Maekawa *et al.*, 1998; Toyama *et al.*, 1999), nectins (Bouchard *et al.*, 2000; Inagaki *et al.*, 2006) and Jam-C/Jam3 (Gliki *et al.*, 2004; Fujita *et al.*, 2007) are expressed on the testicular cells, and their gene-deficient mice show male sterility.

Another IgSF member, RA175 (Cadm1), was first characterised as one of the genes preferentially expressed during the differentiation of P19 mouse embryonal carcinoma cells induced by retinoic acid (Urase *et al.*, 2001; Fujita *et al.*, 2003). The same molecule has been characterised independently and is called by different names: tumour suppressor of lung cancer 1 (TSLC1) (Kuramochi *et al.*, 2001); immunoglobulin superfamily member 4 (IGSF4) (Gomyo *et al.*, 1999); spermatogenic immunoglobulin superfamily member (SgIGSF) (Wakayama *et al.*, 2001); synaptic cell adhesion molecule (SynCAM) (Biederer *et al.*, 2002) and nectin-like molecule 2 (Necl2) (Shingai *et al.*, 2003). These facts indicate the diverse functions of the molecule RA175. RA175 has three immunoglobulin domains in its extracellular region that are involved in cell–cell adhesion via a homophilic or heterophilic interaction (Masuda *et al.*, 2002; Fujita *et al.*, 2003; Wakayama & Iseki, 2009). In order to elucidate the functions of RA175, we have generated mice lacking the gene and found that the resulting $RA175^{-/-}$ male mice were infertile, showing oligoasthenoteratozoospermia

© 2011 Blackwell Verlag GmbH

(Fujita *et al.*, 2006). *RA175*$^{-/-}$ females and heterozygous mice were fertile and no obvious defects were observed. Mice deficient in this gene were subsequently reported by other groups (Surace *et al.*, 2006; van der Weyden *et al.*, 2006; Yamada *et al.*, 2006), and their results agreed with our previous report (Fujita *et al.*, 2006).

In this study, we investigated the location of RA175 in the testis in detail and the characteristics of *RA175*$^{-/-}$ mice to understand the function of RA175. Furthermore, the location of other IgSF members, such as basigin, nectin-2 and nectin-3, which play important roles in spermatogenesis, was examined in the *RA175*$^{-/-}$ testis.

Materials and methods

Animals and antibodies

The generation of mice with the targeted disruption of the *RA175* gene has been previously reported (Fujita *et al.*, 2006). Animal handling was approved by the Animal Research Committee of Chiba University. More than 10 *RA175*$^{-/-}$ and *RA175* $^{+/+}$ mice (3–6 months old) were examined in this study, and more than five sections were analysed per mouse by immunohistochemistry and indirect immunofluorescence. Anti-RA175 antibody was raised against a peptide corresponding to the C-terminal region of RA175, as described previously (Fujita *et al.*, 2003). Goat anti-basigin antibody (sc-9757) and goat anti-nectin-2 antibody (sc-14799) were purchased from Santa Cruz Biotechnology, Inc. (Santa Cruz, CA, USA), and rat monoclonal antibody against nectin-3 was obtained from Abcam (Cambridge, UK). The rat monoclonal antibody TRA98 was a gift from Dr Nishimune of Osaka University.

Immunohistochemistry

Wild-type mice were anaesthetised with pentobarbital and fixed with Bouin's fluid by perfusion through the left ventricle. Testes were removed, embedded in paraffin, and cut at a thickness of 3 μm. These sections were immunostained with either anti-RA175 antibody, anti-basigin antibody or anti-nectin-2 antibody. Non-specific binding of the antibody was blocked by placing the sections in phosphate buffered saline (PBS) containing 5% normal goat serum or foetal bovine serum for 30 min at room temperature (RT). The sections were then incubated with either rabbit anti-RA175 antibody, goat anti-basigin antibody or goat anti-nectin-2 antibody at 4 °C overnight. After washing with PBS, the samples were incubated with biotinylated goat anti-rabbit IgG (Dako Japan Company, Kyoto, Japan) or biotinylated rabbit anti-goat IgG (Dako) for 1 h, followed by incubation with streptavidin–biotin peroxidase complex solution (Dako) for 30 min. Immunohistochemical reactions were visualised using 3,3′-diaminobenzidine and H_2O_2. Several adjacent sections were stained with periodic acid Schiff (PAS) and counterstained with haematoxylin to determine the stages of the seminiferous epithelium.

Indirect immunofluorescence (IIF)

Wild-type and *RA175*$^{-/-}$ mice were anaesthetised with pentobarbital, and perfused through the heart with 4% paraformaldehyde in PBS. The testes and epididymides were removed and immersed in a fixative for an additional 4 h. They were embedded in OCT compound and cut at a thickness of 20 μm on a cryostat. After blocking the sections for 1 h at RT, the testicular sections were incubated with rabbit anti-RA175 antibody or rat anti-nectin-3 antibody, and the sections from the caput epididymidis were incubated with rat monoclonal antibody TRA98 at 4 °C overnight. The slides were then incubated with Alexa Fluor 488 goat anti-rabbit IgG (0.5 μg ml^{-1}; Invitrogen, Carlsbad, CA, USA) or goat anti-rat IgG (0.5 μg ml^{-1}; Invitrogen) together with propidium iodide (1 μg ml^{-1}; Sigma, St. Louis, MO, USA) and RNase (10 μg ml^{-1}; Sigma) in the blocking solution for 1 h at RT. After washing with PBS, the samples were mounted with PermaFluor (Immunon, Pittsburgh, PA, USA) and observed using a confocal laser scanning microscope (LSM510; Carl Zeiss, Oberkohen, Germany). To stain the actin filaments and nuclei in the testis, the frozen sections were incubated with 0.83 μg ml^{-1} FITC-labelled phalloidin (Sigma), 1 μg ml^{-1} propidium iodide (Sigma) and 10 μg ml^{-1} RNase (Sigma) for 1 h, and observed under a confocal laser scanning microscope.

Transmission electron microscopy

The animals were anaesthetised with pentobarbital and perfused transcardially with 3% glutaraldehyde in HEPES buffer. The testes and epididymides were excised and immersed in the same fixative for 2 h at RT. After post-fixation with 1% OsO_4, the tissues were embedded in epoxy resin. Ultrathin sections were prepared, stained with uranyl acetate and lead citrate, and observed under an electron microscope (JEM 1200EX, JEOL, Tokyo, Japan).

Results

Immunohistochemical localisation of RA175 in the mouse testis

The immunohistochemical localisation of RA175 in the wild-type mouse testis was determined by the enzyme-labelled antibody method (Fig. 1). Paraffin sections of the

testis were immunostained with rabbit anti-RA175 antibody. Adjacent sections were stained with PAS and haematoxylin to identify the stages of the seminiferous tubules (data not shown). The results revealed the stage-specific localisation of RA175 in the testicular germ cells. RA175 immunoreactivity was detected on the cell surface of spermatogonia and spermatocytes until stage IV, although all type A spermatogonia did not exhibit a positive reaction. The immunoreactivity became weak in the pachytene spermatocytes at stage V and was not detected in the pachytene spermatocytes at stage VI through step 4 round spermatids at stage IV. Interestingly, the positive staining reappeared on the cell surface of step 5 spermatids. Staining around the head became weak in step 13 spermatids and then disappeared in step 14 spermatids, whereas immunoreactivity around the cytoplasm was detected. Just before spermiation, immunoreactivity was detected only in the residual bodies. Mature sperm in the cauda epididymidis did not exhibit an immunopositive reaction (data not shown). A detailed examination revealed that the immunopositive reaction was confined to the apical surface of type A spermatogonia and was not detected in the basal surface which is in contact with the basal lamina (Fig. 1g). These results are summarised in Fig. 1h. Control experiments using *RA175*$^{-/-}$ testes revealed no RA175 immunoreaction in the spermatogenic cells.

Localisation of RA175 in the testis detected by IIF

Localisation of RA175 in the testis was also detected by IIF (Fig. 2), and positive reactions was observed in the germ cells within the seminiferous tubules. Germ cells immunostained by the enzyme-labelled antibody method (Fig. 1) were also IIF positive (Fig. 2). In addition, late pachytene spermatocytes to early round spermatids, which did not show a positive reaction by the

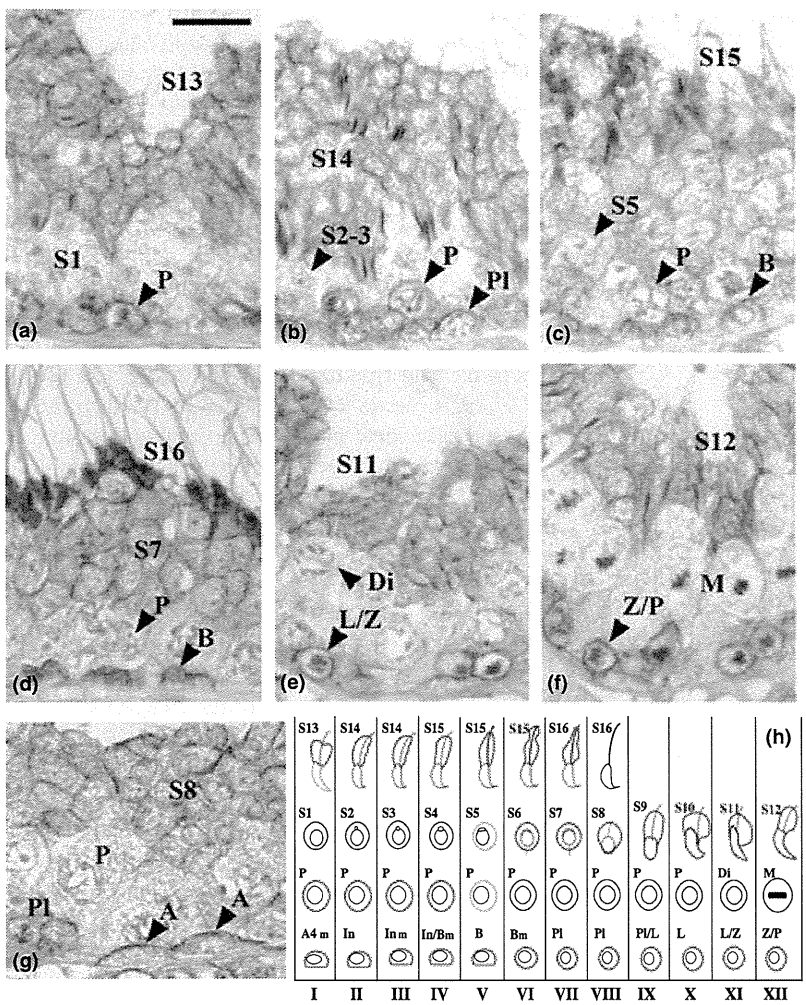

Fig. 1 Immunohistochemical localisation of RA175 in the mouse seminiferous epithelium. (a–g) Paraffin sections of wild-type mouse testes were immunostained with an anti-RA175 antibody (brown) by the enzyme-labelled antibody method and were counterstained with haematoxylin (blue). (a) Stage I, (b) Stage II–III, (c) Stage V, (d) Stage VII, (e) Stage XI, (f) Stage XII. (g) Stage VIII. Bar = 20 μm. (h) Summary of the immunolocalisation of RA175 in the testis. Positive immunostaining is shown in red. A, type A spermatogonia; B, type B spermatogonia; Pl, preleptotene spermatocyte; L/Z; leptotene/zygotene spermatocyte; Z/P, zygotene/pachytene spermatocyte; P, pachytene spermatocyte; Di, diplotene spermatocyte; M, metaphase of the spermatocyte; S1, S2–3, S5, S7, S8, S11, S13, S14, S15 and S16, step 1, 2–3, 5, 7, 8, 11, 13, 14, 15 and 16 spermatid respectively.

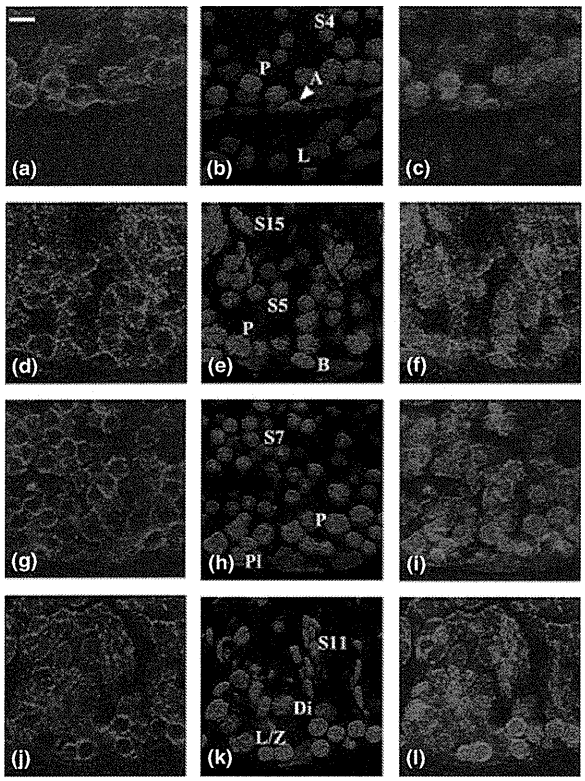

Fig. 2 Immunolocalisation of RA175 in the mouse seminiferous epithelium revealed by IIF. Frozen sections of wild-type testes were immunostained with anti-RA175 antibody (green; a, d, g) and counterstained with propidium iodide for nuclei (red; b, e, h). c, f and I shows merged images. (a–c) Stage IV, (d–f) stage V, (g–i) stage VII, (j–l) stage XI. Bar = 10 μm.

enzyme-labelled antibody method (Fig. 1), were found to be IIF positive. Although reactivity on the cell surface was less distinctive, a diffuse staining in the cytoplasm was revealed by IIF staining (Fig. 2).

Morphological characterisation of the testis and epididymis from *RA175*$^{-/-}$ mouse

Testes from *RA175*$^{-/-}$ mice frequently exhibited abnormal vacuoles in the seminiferous epithelium (Fig. 3a, b). Elongate spermatids were obviously reduced in number in the *RA175*$^{-/-}$ testis. Electron micrographs revealed elongate spermatids with deformed nuclei and/or acrosomes, which were observed frequently in the *RA175*$^{-/-}$ testis (Fig. 3e). An ectopic manchette (Fig. 3f) was often observed; 16 spermatids had irregular manchette out of 44 spermatids. Although the marginal rings of the acroplaxome appeared normal (Fig. 3g), apical ectoplasmic specialisations of the Sertoli cells were separated from the spermatids, and small vacuoles were formed around the spermatids (Fig. 3g, h). This is probably caused by the dissociation of the elongate spermatids from the Sertoli cells through lack of RA175.

Many cells, but not spermatozoa, were found in the epididymis of the *RA175*$^{-/-}$ mouse (Fig. 4). An indirect immunofluorescence study using TRA98 revealed that many cells in the epididymal duct were immunopositive. As the TRA98 antibody recognises germ cells at various stages of differentiation from spermatogonia to spermatids (Tanaka *et al.*, 1997), the positive cells were identified as immature spermatogenic cells and not as spermatozoa (Fig. 4b, d). Round spermatids such as step 3, 5 and 7 spermatids were detected in the epididymal duct by electron microscopy (Fig. 4e, f).

Localisation of basigin, nectin-2 and nectin-3 in the *RA175*$^{-/-}$ testis

To examine the expression of other IgSF members, testes from *RA175*$^{-/-}$ mice were immunostained with anti-basigin, anti-nectin-2 and anti-nectin-3 antibodies (Fig. 5). Basigin was detected in the cytoplasm of round spermatids as well as in the periphery of spermatocytes and spermatids in the wild-type testes (Fig. 5b). In the *RA175*$^{-/-}$ testes, the localisation of basigin was similar to that in the wild-type testes (Fig. 5a). Nectin-2 was localised at the ectoplasmic specialisations of the Sertoli cells, which locates both in the Sertoli–Sertoli junctions of the basal regions (basal ectoplasmic specialisation) and in the Sertoli–spermatid junctions of the adluminal regions (apical ectoplasmic specialisation) of the seminiferous tubules in the wild-type testes (Fig. 5d). In the case of the *RA175*$^{-/-}$ testis, nectin-2 was detected at the basal ectoplasmic specialisations, however, the immunoreaction at the apical ectoplasmic specialisations was not conspicuous, partly because the number of normal elongate spermatids was considerably decreased (Fig. 5c). Nectin-3 was localised in the spermatids adjoining the apical ectoplasmic specialisations in the wild-type testis (Fig. 5f). The spermatids at step 8–9 in the *RA175*$^{-/-}$ testis exhibited a similar nectin-3-immunopositive reaction to the wild-type testis (data not shown). However, at stage XII, when the abnormal morphology of the elongate spermatids at step 12 became noticeable in the *RA175*$^{-/-}$ testis, nectin-3 immunoreactivity was reduced in comparison with that in the wild-type testis (Fig. 5e, f).

An abnormal distribution of actin filaments in the *RA175*$^{-/-}$ testis was revealed by phalloidin staining (Fig. 5g, h). Actin filaments were not observed around the malformed heads of elongate spermatids, and an accumulation of the actin filaments was found in the seminiferous tubules.

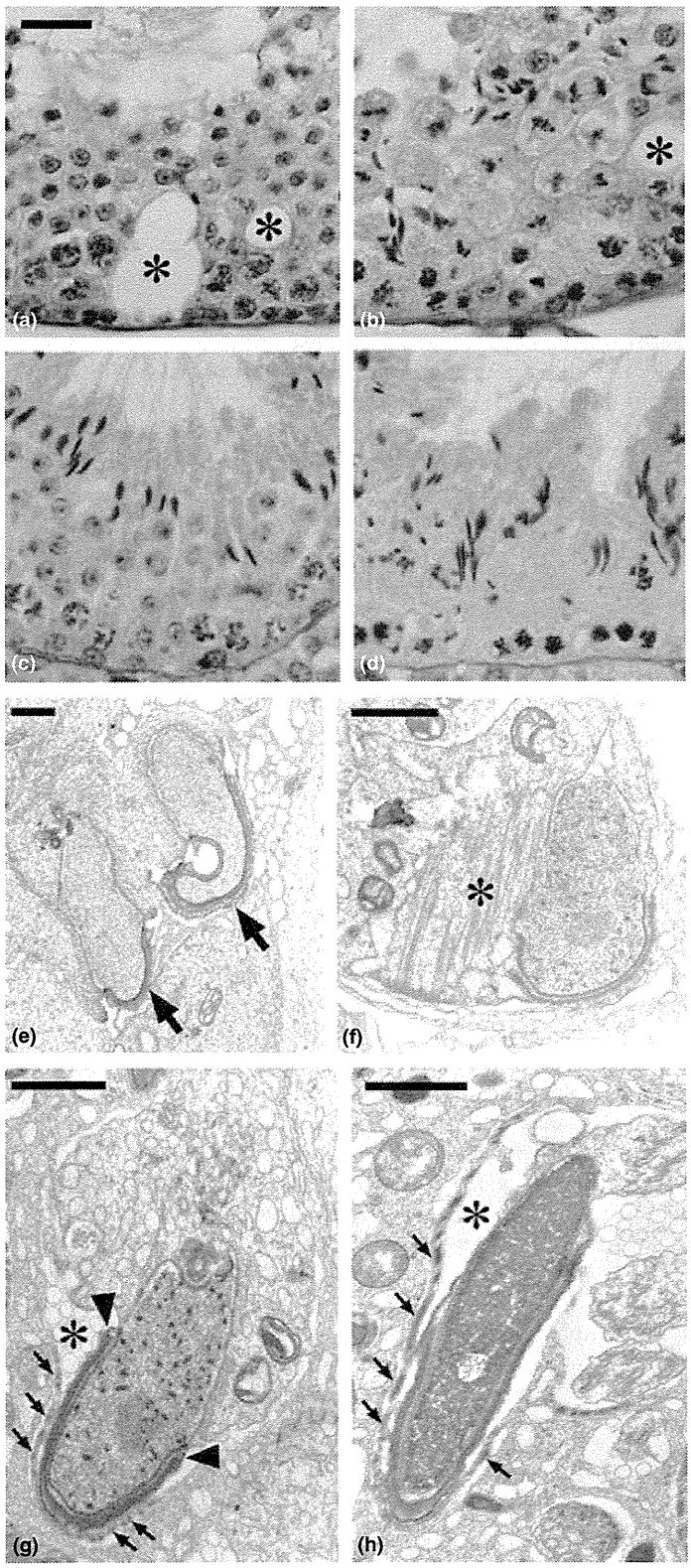

Fig. 3 (a–d) Seminiferous epithelia at stage VI (a, c) and XII (b, d) from *RA175*$^{-/-}$ (a, b) and wild-type mice (c, d) stained with PAS-haematoxylin. The number of elongate spermatids was markedly decreased and vacuoles (*) in the seminiferous tubules were observed in the *RA175*$^{-/-}$ testes (a, b). Bar = 20 μm. (e–h) Electron micrographs of *RA175*$^{-/-}$ testis. Step 9 spermatids with deformed nuclei and acrosomes (e; arrows) and with ectopic manchette (f; asterisk). Small vacuoles (g; asterisk) and dissociation (h; asterisk) between the acrosome of the spermatid and ectoplasmic specialisation (g, h; small arrows) in the Sertoli cell are observed. The marginal rings of the acroplaxome (g; arrowheads) appear to be normal. Bar = 1 μm.

© 2011 Blackwell Verlag GmbH

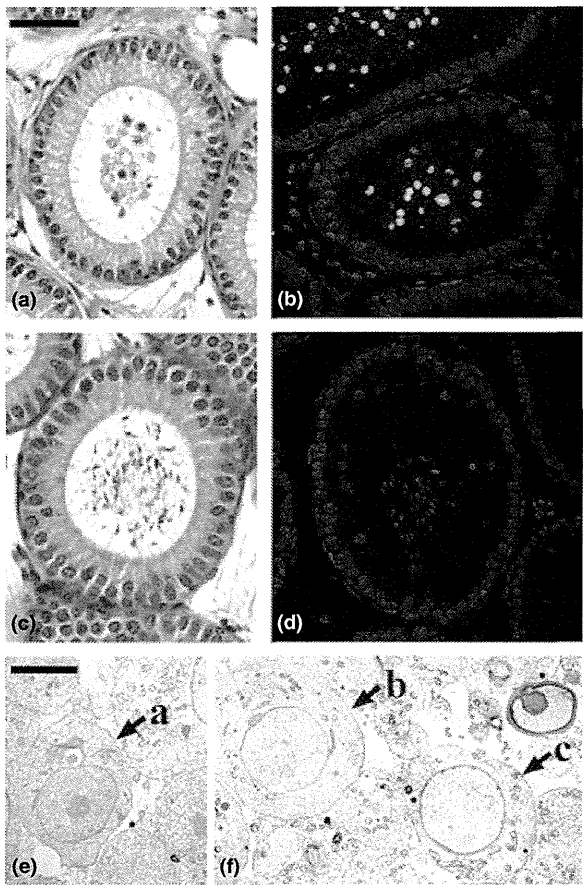

Fig. 4 Caput epididymidis from *RA175*$^{-/-}$ (a, b, e, f) and wild-type mice (c, d). (a, c) Stained with haematoxylin and eosin. (b, d) Immunostained with TRA98 antibody (green) and propidium iodide (red). Bar = 50 μm. (e, f) Electron micrographs of the lumen of the caput epididymidis from *RA175*$^{-/-}$ mouse. Step 3 (a), step 5 (b) and step 7 (c) spermatids were observed in the lumen. Bar = 5 μm.

Discussion

To clarify the function of RA175 during spermatogenesis, it is essential to detect the precise location of this molecule in the testis. Our results in this report (Fig. 1h) revealed a few differences from the previous study (Wakayama *et al.*, 2003; Yamada *et al.*, 2006), which reported that the RA175 protein was detected in spermatogenic cells from intermediate spermatogonia to early pachytene spermatocytes and from step 7 spermatids to the residual bodies of step 16 spermatids. First, we found that several type A spermatogonia were immunopositive for RA175. Spermatogonia are classified either as type A, intermediate, or type B. Type A spermatogonia are the most primitive spermatogonia and are subdivided into undifferentiated (As, Apr and Aal) and differentiating (A1, A2, A3 and A4) spermatogonia (de Rooij & Grootegoed, 1998). As immunonegative type A spermatogonia were also detected, all subpopulations of type A spermatogonia do not express RA175. At present, it is not yet known which subtype(s) of type A spermatogonia express the RA175 protein, however, RA175 can be used as a marker for the differentiation of type A spermatogonia. Secondly, we found RA175 immunoreactivity until pachytene spermatocytes at stage IV, and the reaction diminished thereafter and was not detected from pachytene spermatocytes at stage IV through step 4 spermatids. Subsequently, the activity reappeared in step 5–6 spermatids. Furthermore, by the IIF method, positive reactions for RA175 were detected to some extent in the cytoplasm of mid- to late-pachytene spermatocytes and in round spermatids, which showed no positive staining by the enzyme-labelled antibody method. These differences might be caused by the experimental systems, including the mice strains and antibodies used. However, our IIF results might reflect the intrinsic distribution of RA175, which does not completely disappear during the mid-pachytene spermatocyte to the step 4 spermatid stage.

RA175 immunoreactivity was found at the apical site and not at the basal site of the spermatogonia. This implies that RA175 is localised at the germ cell surface which contacts the Sertoli cells. Thus, it is important to detect the binding partner of RA175 which probably exists in the Sertoli cells. Wakayama *et al.* (2007) identified a poliovirus receptor (PVR) as a binding partner of RA175, which was present in the Sertoli cells of the mouse testis. This finding implies a heterophilic binding between RA175 on germ cells and PVR on the Sertoli cells in the testis.

In *RA175*$^{-/-}$ mice, the number of elongate spermatids was remarkably decreased in the testes, and the remaining elongate spermatids had abnormally shaped heads and acrosomes. Vacuoles were frequently found in the seminiferous epithelium of the *RA175*$^{-/-}$ testis, implying that a cluster of germ cells was exfoliated from the seminiferous epithelium. These observations agreed with those of previous reports (Fujita *et al.*, 2006; van der Weyden *et al.*, 2006; Yamada *et al.*, 2006) and demonstrated that RA175 is responsible for the attachment of germ cells to the seminiferous epithelium and spermatid morphogenesis in the testis. The exfoliated germ cells are partly phagocytosed by Sertoli cells (Fujita *et al.*, 2006), and other cells accumulate in the epididymal duct. It is notable that all germ cells showing RA175-immunopositive reaction were not necessarily exfoliated from the seminiferous epithelium in the *RA175*$^{-/-}$ testis. Other factors probably compensate in part for the function of RA175. Basigin, another IgSF member, exists in these germ cell stages. The molecule was also detected in the